

**CO-EXPOSURE TO UFPM AND O<sub>3</sub>:  
PULMONARY C FIBER AND PLATELET ACTIVATION  
IN DECREASED HRV**

**2017**

**FINAL REPORT  
CONTRACT No. 13-311**

**PREPARED FOR:**

**CALIFORNIA AIR RESOURCES BOARD  
RESEARCH DIVISION  
CALIFORNIA ENVIRONMENTAL PROTECTION AGENCY  
1001 I STREET  
SACRAMENTO, CALIFORNIA 95814**

**PREPARED BY:**

**UNIVERSITY OF CALIFORNIA, DAVIS  
DAVIS, CA 95616**

**SEPTEMBER 14, 2017**

## Project Report

Project Title: Co-exposure to UFPM and O<sub>3</sub>: Pulmonary C fiber and platelet activation in decreased HRV

Agreement No: 13-311

Project Period: September 16, 2013 - September 14, 2017

Submitted to: Patrick Wong  
Research Division  
California Air Resources Board  
1001 "I" Street, 5<sup>th</sup> Floor  
Sacramento, CA 95814

Prepared by: Fern Tablin, Principal Investigator  
Edward Schelegle  
Dennis Wilson

School of Veterinary Medicine  
University of California, Davis  
One Shields Ave.  
Davis, CA 95616

Phone: 530-752-8259

Email: [ftablin@ucdavis.edu](mailto:ftablin@ucdavis.edu)

Disclaimer:

The statements and conclusions in this Report are those of the contractor and not necessarily those of the California Air Resources Board. The mention of commercial products, their source, or their use in connection with material reported herein is not to be construed as actual or implied endorsement of such products.

Acknowledgements:

We thank William Walby and Nghi Nguyen for their technical efforts and expertise. We thank Dr. Joshua Stern for his collaboration.

This Report was submitted in fulfillment of ARB Contract #13-311, Co-exposure to UFPM and O<sub>3</sub>: Pulmonary C fiber and platelet activation by UC Davis under the sponsorship of the California Air Resources Board. Work was completed as of June 30, 2017.

This project is funded under the ARB's Dr. William F. Friedman Health Research Program. During Dr. Friedman's tenure on the Board, he played a major role in guiding ARB's health research program. His commitment to the citizens of California was evident through his personal and professional interest in the Board's health research, especially in studies related to children's health. The Board is sincerely grateful for all of Dr. Friedman's personal and professional contributions to the State of California.

List of Figures:

Figure 1: Lung Histopathology – Terminal Bronchioles and Alveolar Ducts

Figure 2 Lung Histopathology– Terminal Bronchioles and Alveolar Ducts

Figure 3: Lung Histopathology – Large Airways

Figure 4: CD61+ Platelet Microvesicles

Figure 5: NW rats CD11b

Figure 6: SH rats CD11b, CD18 and CD61

Figure 7: Time-varying HRV analysis for time-domain parameters

Figure 8: Time-varying HRV analysis for frequency-domain parameters; LF, HF

Figure 9: Time-varying HRV analysis for frequency-domain parameters; normalized LF, HF and LLF/HF ratio

Figure 10: Ventricular Ectopy Severity Score

Figure 11: Arrhythmia Severity Score

Figure 12: Severity of Supraventricular Complexes

Figure 13: Atrial Premature Complexes

Figure 14: Atrioventricular Block

Figure 15: Severity of Atrioventricular Block

Figure 16: ECG tracing

Figure 17: Histopathology Image Hypercontractility

Figure 18: Histopathology Image Focal Organized Necrosis

Figure 19: Histopathology Image Acute Cellular Necrosis

Figure 20: Cardiac Histopathology: NW vs SH: acute cellular necrosis, hypercontractility and organized focal necrosis

List of Tables:

Table I – Histopathologic Measurements of Lung

Table II - Platelet and White Blood Cell Counts

Table III – Platelet Flow Cytometry

Table IV – Platelet-White Blood Cell Aggregate Flow Cytometry

Table V – Time-varying value SDRR

Table VI – Time-varying values RMSSD

Table VII – Time-varying values HRV triangular index

Table VIII– Time-varying values normalized low frequency

Table IX – Time-varying values for normalized high frequency

Table X – Time-varying values for low frequency: high frequency ratio

Table XI - Histopathologic Measurements of Heart Pathology

## Table of Contents

1. Abstract	5
2. Executive Summary	6
3. Background, Introduction	8
4. Objectives and Methods	10
5. Results	19
6. Summary and Conclusions	51
7. Recommendations	52
8. References	53
9. Glossary of Terms, Abbreviations and Symbols	55

**Abstract:**

Air pollution is composed of a variety of substances including ozone and particulate matter. Historically it has been shown that older people with pre-existing cardiovascular disease are particularly sensitive to air pollution exposure. This study uses mature adult rats with and without pre-existing cardiovascular disease to understand the effects of combined pollutant (ozone and particulate matter) exposure on the cardiovascular and respiratory systems. Our studies demonstrate that both mature adult normal and spontaneously hypertensive animals were most significantly affected by co-pollutant exposures. Mature adult animals with pre-existing cardiovascular disease were more susceptible to oxidant stress of exposure and at greater risk with regard to alterations in the peripheral vasculature and heart and lung tissue as a result of exposure to either ozone or the combination of ozone and ultrafine particulate matter. In the peripheral blood this was reflected in a greater number of platelet-white blood cell aggregates. Pathological changes, including edema, macrophage and neutrophil infiltrates, as well as necrosis in the proximal airways and terminal bronchioles were present in the lungs of spontaneously hypertensive animals exposed either to ozone or combined ozone/ultrafine particulate matter. Similar lesions were seen in the normal Wistar rats but only for the combined pollutants. In both groups of animal's lung injury and inflammation was associated with an increase in heart rate variability that was associated with increased number and severity of arrhythmias and an increase in parasympathetic outflow to the heart. Both strains of rats exposed to ozone + ultrafine particulate matter had significant differences in the severity of ventricular entropy, severity of arrhythmias and ventricular pre-contractions as well as total number of atrial-ventricular block events when compared to filtered air exposed animals. Only, in the spontaneously hypertensive rats were the changes in heart rate regulation and arrhythmias associated with acute myocardial cellular necrosis, hypercontractility and focal myocardial organized necrosis. When comparing the two strains of rats there were significantly greater severity scores for all myocardial histopathologic parameters in the spontaneously hypertensive animals exposed to combined pollutants. Our data is consistent with the combined pollutant atmosphere being more toxic than would be expect from the responses elicited by ozone and ultrafine particulate matter alone and with chronic cardiovascular disease increasing the susceptibility to pollutant induced lung and heart injury. This information provides us with a better understanding of the mechanisms responsible for increased deaths associated with older people with underlying cardiovascular disease in response to significant air pollution exposure.

## 2. Executive Summary:

### *BACKGROUND:*

Many observational and epidemiological studies have consistently demonstrated that exposure to particulate matter (PM) is associated with increased cardiovascular (CV) morbidity and mortality. This is particularly true for people with underlying cardiovascular disease (CVD) including but not limited to: hypertension, atherosclerosis, angina and myocardial infarction. Furthermore, short term (acute) PM exposures have been associated with excess deaths from myocardial ischemia, heart failure and arrhythmias (Samet et al. 2000, Peters et al., 2001). Understanding of the mechanisms responsible for increased cardiovascular risk, especially in older populations is critical to the mission of the ARB. These data will aid in the development of air pollution regulatory strategies.

### *OBJECTIVES AND METHODS:*

Mature adult animals with and without pre-existing CVD were used in this study to mirror the epidemiologic data described above. Prior to the study, animals were instrumented with telemeters to enable us to study the animal's electrocardiogram while awake and with freedom of movement. Once animals recovered from surgery (minimum two-week recovery period) animals were exposed to filtered air (FA), ultrafine particulate matter (UFPM), ozone (O<sub>3</sub>) or co-pollutant ultrafine particulate matter and ozone (UFPM+O<sub>3</sub>) for 6 hours followed by an 8-hour recovery period prior to euthanasia. Electrocardiographic (ECG) data were obtained through the exposure and recovery periods, and assessed for the appearance of arrhythmias and measures of heart rate variability (HRV). The study was performed at the University of California, Davis in 2015-2017, under IACUC approved protocols. Both peripheral blood and tissues were obtained at the time of euthanasia for further analysis. Flow cytometry was used to determine platelet activation as well as platelet-white blood cell interactions; a reflection of systemic inflammation. Lung and heart tissue was analyzed to determine if there were adverse effects associated with exposure.

### *RESULTS:*

Our study showed that mature adult animals with pre-existing CVD were more susceptible to oxidant stress of exposure and at greater risk with regard to alterations in the peripheral vasculature as well as in the heart and lung tissue as a result of exposure to either O<sub>3</sub> or UFPM+O<sub>3</sub>. In the peripheral blood this was reflected in a greater number of platelet-white blood cell aggregates. Pathological changes, including edema, macrophage and polymorphonuclear (PMN) leukocyte (neutrophil) infiltrates, as well as necrosis in the proximal airways and terminal bronchioles were present in the lungs of spontaneously hypertensive animals exposed either to O<sub>3</sub> or UFPM+O<sub>3</sub>. Similar lesions were seen in the normal Wistar rats but only in response to UFPM+O<sub>3</sub>. In both groups of animals' lung injury and inflammation was associated with a decreased HRV that associated with increased number and severity of arrhythmias and an increase in parasympathetic outflow to the heart. Both strains of rats exposed to UFPM+O<sub>3</sub> had significant differences in the severity of ventricular entropy, severity of arrhythmias and ventricular pre-contractions as well as total number of atrial-ventricular block events when compared to filtered air exposed animals. Only in the spontaneously hypertensive rats were the changes in heart rate regulation and arrhythmias associated with pathological changes in the myocardium including acute cellular necrosis, hypercontractility and focal organized necrosis. When comparing the two strains of rats there were significant differences between the strains for all 3 parameters in UFPM+O<sub>3</sub>-exposed animals.

*CONCLUSIONS:*

These data provide critical information regarding the risks of combined pollutants (UFPM+O<sub>3</sub>) in mature adults with underlying CVD as well as mechanisms of disease in these populations. Our data is consistent with the combined pollutant atmosphere being more toxic than would be expect from the responses elicited by O<sub>3</sub> and UFPM alone and with chronic CVD increasing the susceptibility to pollutant-induced lung and heart injury. This will aid CARB in developing and evaluating air pollution standards.

## 2. Background and Introduction:

The pathways by which UFPM exerts CV effects can be divided into two different areas. In the first pathway, the pulmonary system has been shown to respond to UFPM through the production of systemic pro-inflammatory and pro-thrombotic cytokines. Thus, indirectly leading to downstream events, including production of acute phase proteins CRP and plasma fibrinogen. This pathway has been borne out by human clinical studies as well as numerous animal studies including CAPs studies from our laboratory (Wilson et al., 2010; Tablin et al., 2012). The development of a pro-thrombotic and/or pro-coagulable state requires release of pro-inflammatory factors into the pulmonary vasculature leading to downstream activation of both the vascular endothelium and blood platelets. Human and animal studies of inhaled concentrated UFPM has been shown to result in increases in platelet activation, platelet-leukocyte and platelet-monocyte interactions (Lucking et al., 2008) as well as decreased fibrinolysis – all of which are predisposing factors for thrombus formation potentially resulting in myocardial ischemia.

A second pathway by which UFPM can exert their CV effects is the direct translocation of fine and ultrafine PM into the pulmonary circulation. This has been convincingly demonstrated in animal models (Oberdorster et al., 2002), but direct evidence in humans appears lacking. Movement of UFPM directly into the circulation allows for direct interactions with blood cells and the vascular endothelium. While a variety of factors determine which elements of UFPM are able to cross the alveolar wall, the end result can be similar to that of indirect pulmonary effects; increased systemic inflammation. There is considerable data to suggest that circulating UFPM also can interact with and destabilize atherosclerotic plaques leading to their rupture, the develop of thrombi, and acute coronary syndrome (Brook et al., 2004). Studies in ApoE<sup>-/-</sup> mice demonstrated increased number and sizes of aortic plaques, in association with UFPM; rich in polycyclic aromatic hydrocarbons (PAHs) (Araujo et al., 2008).

Regardless of the pathway, UFPM can exert their effects directly or indirectly on the autonomic nervous system leading to altered heart rate variability (HRV). There is a well-documented relationship between the ability of the autonomic nervous system to regulate the cardiac cycle and CV mortality (Malik et al., 1996). Alterations in HRV have been demonstrated in both short term and chronic UFPM exposures. Studies by Fan and colleagues (2009) demonstrated that acute UFPM exposure in healthy older adults results in acute decline in the ratio of low frequency to high frequency components of heart rate indicating increased parasympathetic input to the heart. The elderly, with and without ongoing CVD, are among the largest of the affected populations (Adar et al., 2007; Pope et al., 2004). A meta-analysis study by Pieters and colleagues (2012) concluded that there is “an inverse relationship between HRV, a marker for a worse CV prognosis, and particulate air pollution.”

Human UFPM exposure studies provide clear indications of association with systemic inflammation, platelet activation, and the increase in acute phase proteins (Delfino et al., 2008). Some of the most pronounced effects were seen with UFPM. Studies with wood smoke and cigarette smoke have suggested that these pollutants activate pulmonary C fibers, releasing neurokinins that affect both the systemic circulation and the autonomic nervous system, resulting in a reflex reaction that eventually leads to altered HRV.

Due to the close association, both temporally and geographically, of O<sub>3</sub> and UFPM, it has been difficult to separate the effects of these two pollutants. Animal model studies have shown that O<sub>3</sub> acts through biochemical modification of airway surface liquid to form oxidative intermediates that injure airway epithelial cells, and selectively targets ciliated cells of the upper airways and terminal bronchiolar regions for degeneration and necrosis. O<sub>3</sub>-induced airway injury has been shown to be associated with C fiber pathway activation (Schelegle et al., 2001). There is limited literature in this regard, despite the potential for this pathway to induce alterations in heart rate regulation. However, a recent experimental study of healthy human subjects by Devlin and colleagues (Devlin et al., 2012) has demonstrated that O<sub>3</sub> can result in

increases in systemic inflammation, fibrinolysis and autonomic dysfunction markers, similar to those seen in association with UFPM exposure.

Despite the fact that air pollution is frequently a mixture of UFPM and O<sub>3</sub>, there are few studies examining their individual and synergistic effects. Studies of co-pollutant exposures demonstrated altered vagal tone (a short term autonomic imbalance) resulting in a reduced ratio of low frequency to high frequency components of heart rate (Gold et al., 2000). Work by Brook and colleagues (Brook et al., 2002) in healthy adults, demonstrated that co-exposures resulted in acute arterial vasoconstriction, which could, particularly in patients with CV disease, promote myocardial ischemia.

### 3. Objectives and Methods:

#### Objectives:

- Surgical Implantation of Telemetry Units into Normal Wistar and Spontaneously Hypertensive Wistar Rats
- Prior to Exposures Collect Peripheral Blood for Analysis of Platelet and White Blood Cell (WBC) parameters
- Exposure of Instrumented Normal Wistar Rats to filtered air (FA; n=10), ozone (O<sub>3</sub>; n=9), ultrafine particulate matter (UFPM; n=8) and UFPM+O<sub>3</sub> combined (n=11). Electrocardiographic data were recorded throughout exposure.
- Exposure of Instrumented Spontaneously Hypertensive Wistar Rats to filtered air (n=12), UFPM (n=10), O<sub>3</sub> (n=8) and UFPM+O<sub>3</sub> combined (n=12). Electrocardiographic data were recorded throughout exposure.
- Post-exposure Blood Collection, Euthanasia, Collection of Tissues for Histology.

#### A. Particle and Ozone Generation:

*Particle generation.* Particles employed were described previously (Lee et al., 2010). Briefly, pre-mixed flame particles (PFP) were generated by an annular tubular burner. An ethylene, oxygen, and argon mixture flowed through the 0.71 cm inside diameter center of the burner stabilized by an outer annulus of oxygen. Flow rates of each gas were calculated to achieve a total flow of 2 L/min while maintaining an estimated adiabatic flame temperature of 1900 K. Equivalence ratios,  $\phi$ , was equal to 2.2. The flame was surrounded by a nitrogen jacket flowing at 10 L/min to prevent oxidation of the particles. Gas flow rates for ethylene, oxygen and argon were metered by mass flow controllers with a full-scale accuracy of 2% and typical flows were at 50% of full scale. Air and nitrogen flows were metered by rotometers. A three-way automobile catalyst oxidized carbon monoxide and hydrocarbons to carbon dioxide and reduced oxides of nitrogen to oxygen and nitrogen. FA was added downstream of the flame to provide oxygen for the catalyst. All flame products were then mixed with high efficiency particulate air filtration HEPA/CBR (Chemical Bacteriological Radiological)-FA metered to obtain desired dilution ratio.

Particle size distribution and number concentration were measured in the exposure chamber using a TSI 3071 SMPS (Scanning Mobility Particle Sizer) or TSI 3775 CPC (Condensation Particle Counter). The TSI 3071 uses a 0.0457-cm impactor, a long DMA (Differential Mobility Analyzer, TSI 3081) and a 3010 CPC. A sample was drawn onto glass-fiber filters (Pall Corp., NY) from the exposure chamber during each exposure for 120 min at 20 L/min and weighed to determine average mass concentration. Using data from a series of UFPM and UFPM+O<sub>3</sub> exposures, the exposure chamber mass concentration was determined to be  $253.1 \pm 7.28 \mu\text{g}/\text{m}^3$  UFPM (mean  $\pm$  SD) based on gravimetric filter measurement. SMPS measurements showed a geometric mean mobility diameter of 74.14 nm with a geometric standard deviation of 1.26 nm. The mean particle number concentration was  $1.57 \times 10^5 \pm 3.6 \times 10^3$  particles/cm<sup>3</sup> (mean  $\pm$  SD) based on CPC measurements over duration of exposure. Exposure chamber CO and CO<sub>2</sub> levels were within 0.3 ppm of FA chamber levels, with quantification below 0.2 ppm limited by instrument accuracy. Particles were high in organic carbon and had an EC/OC ratio of 0.58. The mass concentrations used in this study were higher than typical ambient UFPM values and levels were determined in consultation with ARB staff. It is important to remember that rats are obligate nose breathers and are highly efficient nasal scrubbers. Thus, the concentration of UFPM was chosen as a dose having a high

likelihood of having a biological effect. Differences between human and animals in particle clearance, deposition pattern, and biological response to toxicants should be considered for proper interpretation of results, however it is important to recognize that the level of UFPM in this study is not out of the realm of a high actual exposure.

*Ozone generation.* Ozone (O<sub>3</sub>) was generated as described previously (Schelegle et al., 2001) by passing oxygen through an ozonizer (model 100, Sanders, Uetze-Eltze, Germany). After being mixed with filtered air, the gas was delivered (10 l/min) to the top compartment of the exposure chamber. All flows will be controlled using mass flow controllers (Tylan General). The concentration of ozone was kept constant using a proportional controller (Inhalation Facility, University of California, Davis, California Regional Primate Research Center, Davis, CA) interfaced with an ultraviolet ozone analyzer (model 1003-AH, Dasibi Environmental, Glendale, CA). The ozone analyzer is routinely calibrated using the ultraviolet absorption photometric method at the University of California, Davis, California Regional Primate Research Center.

## **B. Telemetry System and ECG Recording:**

*Telemetry system and Electrocardiograph (ECG) recording.* A telemetry-based biopotential amplifier and transmitter system (Telemetry Research Auckland, New Zealand) was utilized to measure ECG signals. The unit incorporates an amplifier, 12-bit analog-to-digital converter sampling at 2 kHz, and transmitter (2.4-GHz band, range 5 m). The transmitter was encapsulated in medical-grade silicone and measured 35 × 23 × 11 mm, with a weight of 13 g. A receiver was responsible for reconstructing the transmitted data signal. The typical range was 5 m. The ECG signal from the transmitter was received via a dedicated receiver (Telemetry Research). This signal was band-pass filtered between 1 and 2,000 Hz, and the reconstructed analog signal was displayed using a PowerLab data-acquisition system (sampling at 4,000 Hz) with associated LabChart software (model ML870, ADInstruments, North America). The ECG signal was further analyzed using the Kubios Heart Rate Variability Premium 3.0 for Macintosh (Kubios, Kuopio, Finland).

## **C. Experimental Animal Models and Surgical Procedures, Animal Exposures:**

*Animal Models.* Normal (NW) and spontaneously hypertensive (SH) male Wistar-Kyoto rats (350-700 g) mature adult (10-14 mos) were delivered from the vendors (Charles River and Envigo Laboratories). Animals were housed in filtered air chambers in American Association for Accreditation of Laboratory Animal Care-approved facilities. All procedures were part of an Institutional Animal Care and Use Committee-approved animal protocol.

*Surgical Procedures.* Animals were allowed to acclimate in vivarium for at least five days prior to undergoing surgical procedures. Rats were fasted for a minimum of 12 hours prior to surgery. Rats were then placed in a 10 liter glass chamber and anesthesia was induced by 5% isoflurane induction and maintained through surgical procedures with 3-5% isoflurane (Abbott Laboratories, U.S.A.). A 0.1 to 0.5 ml blood sample was then obtained from a tail vein and analyzed for platelet and white blood cell counts. Following blood draw the rats were treated with meloxicam (2 mg/kg, SQ) and enrofloxacin (5 mg/kg, IM) and ophthalmic lubricant was applied to each eye. Abdominal, intercostal and femoral regions were shaved and skin surfaces were deeply scrubbed with a betadine solution. Following these injections and at least 10 minutes prior to surgery the incision sites were treated with multiple small subcutaneous injections of bupivacaine (5mg/ml, total volume did not exceed 0.25 ml). A 4-5 cm midline abdominal incision was made in skin starting at the xiphoid and subcutaneous channels for the telemeter leads were formed using blunt dissection. A 2.0-2.5 cm incision was then made in the linea alba again starting at the xiphoid. A two-lead biopotential telemeter (TR50B Millar, Inc) was then placed in the abdominal cavity and secured to the lower abdominal wall using soluble suture. The incision in the linea alba was closed using monofilament suture and 10-15 cm of telemeter lead wire exited the closed incision near the xiphoid. The telemeter leads were

secured using silk suture to the fascia covering the cranial portion of the sternum and the right eighth to tenth rib dorsal to the insertion of rectus abdominis, and the quality of the ECG signal examined. These sites were chosen to minimize artifact associated with breathing and movement and produced a signal similar to an aV2R ECG lead. Each surgical procedure lasted approximately 45 minutes. During recovery, animals were placed in a heated cage at approximately 37°C and were then individually housed in standard rat cages after their health condition was assured. During the recovery period, the animals were monitored twice daily and analgesic therapies (see above) as well as buprenorphine (Buprenorphine (0.03 mg/kg), Par Pharmaceutical) was administered twice daily for two days post-surgery. Animals were allowed at least 14 days recovery prior to experimental procedures.

*Animal Exposures.* On the day of study, animals were transferred into a standard rodent cage with an open wire mesh top with a perforated Teflon plate inserted ~1 inch above bottom of the standard cage. Animals were placed in exposure chamber at least 1 h prior to exposure protocol. Animals were exposed to one of the following exposure conditions: (1) filtered air (FA); (2) 1ppm; O<sub>3</sub> (3) 250-300 µg/m<sup>3</sup> UFPM, and (4) 1.0 O<sub>3</sub> and 250-300 µg/m<sup>3</sup> UFPM. The exposure protocol was: (1) 60-minute control period, (2) 6-hour exposure period, and (3) 8-hour recovery period. Exposure protocol duration was based on historical O<sub>3</sub> exposure studies, where the O<sub>3</sub> levels produced moderate oxidant injury lesions in young adult rats. The recovery time was designed to be sufficient for the development of neutrophilic inflammation and presentation of injury (Pino M.V. et al., 1992). ECG signals were collected continuously through the exposure protocol. Animals were euthanized following exposure protocol.

#### **D. Cardiopulmonary Pathology:**

*Methods.* Lungs and heart were fixed by intratracheal instillation of neutral buffered formalin with a controlled pressure of 20 cm H<sub>2</sub>O.

*Lung:* Three lung sections from each animal were paraffin embedded, sectioned, and stained with hematoxylin and eosin. Proximal and distal sections of the left lobe were selected in a plane perpendicular to the first axial airway. The third section was a transverse section of the accessory lobe that also included its main axial airway.

*Heart:* The heart was bisected from the base to apex in a plane including both right and left ventricles and atria. Standard, paraffin-embedded, hematoxylin and eosin histopathology sections were prepared and coded by random sequencing.

*Histopathology scoring.* Sections were evaluated by a veterinary pathologist without knowledge of treatment group assignment. In the lung, lesions in large airways, terminal bronchiolar/alveolar duct regions, alveolar parenchyma and vasculature were assigned a severity score from 0-5 based on the extent and density of cellular debris and inflammatory cell responses in each section examined. Numerical scores correlated with normal (0) minimal (1) mild (2) moderate (3) severe (4) and maximal (5) responses. For the lung, lesion scores were separately assigned for edema, neutrophil infiltrate, macrophage infiltrate, epithelial necrosis, large airway ciliary cell loss/necrosis and intravenous fibrin/neutrophil aggregates. For the heart, separate severity scores were recorded for focal organized necrosis (FON), acute cellular necrosis (ACN), and hyper-contractility (HC).

*Statistical Analysis.* Histopathologic scores were assessed for significance using a nonparametric Kruskal-Wallis test, with Dunn-Bonferroni post-hoc comparisons to identify significant differences between each exposure group and FA by strain. Additionally, the nonparametric Mann-Whitney test was used to identify significant differences between strains in response to each exposure.

### **E. Hematology, Platelet and White Blood Cells:**

Prior studies from our laboratory (Wilson et al., 2010) and those of Lucking et al. (2008) and others has shown that inhalation of PM results in platelet activation as well as platelet-neutrophil aggregates. Both activation and the presence of aggregates contributes to increased thrombin formation in humans and mice; thus, we chose to examine those parameters in this study as well.

*Hematology.* Baseline blood samples were collected from the tail vein under institutionally approved protocols, into acid citrate dextrose (ACD)-coated syringes with a ratio of 1:10 ACD: blood. Post-exposure blood, from the inferior vena cava was obtained before the animals were euthanized. Whole blood was incubated at 37°C for 30 min prior to use. Platelet and white blood cell (WBC) counts were determined using an automated blood counter (ActDiff, Coulter, Miami, FL).

*Platelet activation analysis.* Rat platelet activation was analyzed in whole blood by flow cytometry using three monoclonal anti-rat antibodies. For all platelets studies, whole blood was diluted in Tyrode's Hepes with 5mM dextrose pH7.2 (Norris et al., 2006) to a final platelet count of  $1 \times 10^6/\mu\text{l}$ . The major platelet integrin  $\alpha_{2b}\beta_{3a}$  was evaluated with a phycoerythrin (PE)-conjugated monoclonal antibody to the  $\beta_{3a}$  subunit (CD61) (BD Pharmingen). Alpha granule secretion was evaluated with a fluorescein isothiocyanate (FITC)-conjugated monoclonal antibody to P-selectin (CD62P) (BD Pharmingen), and lysosomal granule secretion was evaluated with a PE-conjugated monoclonal antibody to a lysosomal membrane protein (CD63) (eBioscience). An isotype control was used for each antibody. Two populations of platelets were examined for each animal, a resting (unstimulated) sample and a sample stimulated with 0.1 U/ml thrombin (15 min room temperature). After stimulation of whole blood, platelets were labeled with the preceding antibodies for 1 h and fixed in 1% (final) paraformaldehyde prior to analysis by flow cytometry. Platelets were defined by forward (FSC) a measure of size, and side scatter (SSC) a measure of cellular density, characteristics and ten thousand events were collected within the platelet gate for each animal and each condition. Platelet-derived (CD61-positive) membrane microvesicles were identified based on forward scatter (FSC), with the x-axis threshold set at  $10^1$ , representing the lower FSC boundary for unstimulated platelets.

*White Blood Cell – Platelet Aggregate Analysis.* Whole blood was diluted in Tyrode's Hepes with 5mM dextrose pH7.2, to a final white blood cell (WBC) count of  $1 \times 10^3/\mu\text{l}$ . Diluted blood was labeled with antibodies to either CD61 (platelets) and CD11b (WBC integrin  $\alpha_M$ ) or CD61 and CD18 (WBC integrin  $\beta_2$ ). Samples were fixed in FACs-lyse (Becton Dickinson) for 1 hour prior to flow cytometric analysis. Five thousand CD11b or CD18 positive events were collected for each sample.

*Flow Analysis.* All samples were examined on a Beckman Coulter FC500 and analyzed in FlowJo (TreeStar Ashland, Oregon). FMO (fluorescence minus one) were used to set compensation for all samples. Percent positive cells and mean fluorescence intensity were evaluated for all samples.

### **F. Heart rate variability analysis:**

Heart rate variability (HRV) is defined as the regularity, or lack thereof, of the timing between successive heart beats. HRV is examined using three general approaches, time-domain analysis, linear spectral analysis and non-linear spectral analysis. The time-domain methods are the simplest to perform and generate since they are applied to a series of successive RR interval values and utilized commonly recognized statistical parameters such as standard deviation and square root of the mean squared differences. Time-domain parameters therefore provide information about how variable heart rate is over a given sampling period. Both linear and non-linear spectral approaches examine the complex signal generated by plotting the RR interval against time. Linear spectral analysis views the RR interval-time signal as being

composed of multiple frequencies and uses various approaches to extract this frequency domain information. Regardless of the approach it is possible to identify within the derived frequency domain information very low, low, and high frequency components (VLF, LF and HF). This information is useful because LF and HF are both influenced by autonomic nervous system regulation of heart rate, with an increase in HF or a decrease in the LF/HF ratio indicating an increase in parasympathetic input to the heart. Though somewhat misleading changes in the LF/HF ratio is often used to determine whether HRV decreases in exposure studies, even though parameters of time-domain analysis may at the same time increase. Non-linear analysis examines the fractal dimensionality of the RR interval-time signal and provides parameters that have been shown to correlated with frequency domain endpoints. Several clinical studies have demonstrated that there is a direct correlation between alterations in specific parameters of HRV and subsequently poor medical outcomes. To better understand this relationship in the context of air pollution exposure and CVD, we examined specific time- and frequency-domain measures of HRV following guidelines described previously (International Task Force 1996).

*Time-domain Methods.* In a continuous electrocardiographic (ECG) record, each QRS complex was detected, and the so-called R-to-R (RR) intervals (that is all intervals between adjacent QRS complexes resulting from sinus node depolarizations), were determined. Time-domain measures were computed using statistical and geometric methods from the de-trended RR (Table 1).

Table 1. Time-domain Measures

Measure	Units	Definition	Conventional Interpretation
SDRR	ms	Standard deviation of RR intervals	Represents all the RR-interval variability present during the included sample time
RMSSD	ms	Square root of the mean squared differences between successive RR intervals	Estimate of short-term components of HRV, reported to reflect parasympathetic nervous system input
HRV triangular index		The integral of the RR interval histogram divided by the height of the histogram	Expresses overall HRV measured during sample times and is more influenced by the lower frequencies

*Frequency-domain Methods.* For methods of frequency-domain analysis, a power spectrum density (PSD) estimate is calculated for the RR interval series. In HRV analysis, the PSD estimation can be carried out using either fast Fourier transform (FFT)- or parametric autoregressive (AR) modeling-based methods. The advantage of FFT based methods is the simplicity of implementation, while the AR spectrum yields improved resolution especially for short samples. Another property of AR spectrum is that it can be factorized into separate spectral (i.e., VLF, LF, and HF) components. The disadvantages of the AR spectrum are the complexity of model order selection and the contingency of negative components in the spectral factorization. We collaborated with Dr. Mika Tarvainen, a well-published expert on HRV, to determine the model order number that “best fit” the data and removed negative components from the spectral factorization.

The generalized frequency bands in case of short-term HRV recordings are the very low frequency (VLF, 0–0.04 Hz), low frequency (LF, 0.04–0.15 Hz), and high frequency (HF, 0.15–0.4 Hz). In the FFT spectrum, power values for each frequency band are obtained by simply integrating the spectrum over the band limits. Alternatively, in the AR spectrum, spectral factorization enables distinct spectral components to emerge for each frequency band with a proper selection of the model order and the absolute power values are obtained directly as the powers of these components. Thus, it is a more accurate measure of power distribution.

The frequency-domain measures of LF and HF peak component powers were computed from the de-trended and interpolated (equidistantly sampled) RR interval series (Table 2). LF and HF powers were also computed in normalized units (n.u.), which were obtained by dividing the absolute powers with total spectral power and multiplying by 100 to give values as a percentage (Table 2). The frequency-domain measures were calculated from the RR interval spectrum, which was estimated using autoregressive (AR) spectrum estimation with model order 18.

Table 2. Frequency-domain Measures

Measure	Units	Definition	Conventional Interpretation
LF Peak	Hz	Peak power in low frequency range within selected time frame	Used in time-varying analysis to demonstrate change over selected time-frame
HF Peak	Hz	Peak power in high frequency range within selected time frame	Used in time-varying analysis to demonstrate change over selected time-frame
LF	n.u.	Normalized unit of power in the low frequency range	Sympathetic response
HF	n.u.	Normalized unit of power in the high frequency range	Parasympathetic response
LF/HF		Ratio between LF and HF band powers	Relative balance of sympathetic to parasympathetic responses

*Time-varying Methods.* Time-varying analysis was used to demonstrate the trends in time- (SDRR, RMSSD, HRVti) and frequency- (peak frequencies and/or band power for LF, HF, and LF/HF ratio) domain measures throughout the exposure protocol. The trends of the frequency-domain measures were computed based on a time-varying spectrum estimated using the Kalman smoother algorithm (Tarvainen et al., 2006).

*Statistical Analysis.* The effect of exposure on HRV time and frequency domain parameters were determined by mixed model three-way analysis of variance (ANOVA) with repeated measures ( $p < 0.05$ ) using procedures described previously (8). There are two steps for performing a mixed model three-way ANOVA with repeated measures. First, we determined the best fit of the data to one of multiple within-subject covariance structures using the Akaike information criterion (AIC) and the Schwarz Bayesian criterion (SBC) to determine which covariance structure best fit the data. Both the AIC and the SBC indicated that the unstructured covariance structure best-fit the data. Second, we analyzed the data for time and exposure effects on HRV by estimating and comparing means using a Bonferroni adjustment (IBM SPSS Software; IBM Analytics, Armonk, New York).

## **G. Electrocardiographic Analysis, Assessment was conducted by Joshua Stern, DVM, PhD, DACVIM (Cardiology):**

*Methods.* 14-15 hours of continuous ECG recording was reviewed using LabChart v8.1.3 for Mac. A single trained investigator (veterinary cardiologist, JAS) was blinded to subject strain and exposure group. Each file was reviewed first in Scope View for periods of irregularities at high speed (30x) and later by prospective beat-by-beat evaluation. Complexes that were not identified as either normal sinus or artifact were classified and recorded by type and characteristic of arrhythmia (ECG glossary provided below). Ultimately, arrhythmias were divided based on origin, into three categories, ventricular ectopy, supraventricular ectopy or atrioventricular block. Scoring systems are detailed below.

### **ECG Glossary**

Ventricular Premature Complexes (VPC) – A premature complex that is conducted from the ventricle and is thus wide and bizarre when compared to the surrounding normal sinus complexes. VPCs often incite a compensatory pause immediately after they are conducted.

Polymorphic Ventricular Premature Complexes (P-VPCs) – VPCs that have varied morphology. P-VPCs are noted when the sinus complexes remain of constant morphology, yet the VPCs observed are of different morphology. This suggests a different ectopic focus in the ventricular myocardium. As the ECG tracings may change with body position, the investigators required that the sinus impulses remain of constant morphology surrounding the VPCs if the determination of polymorphic origins was made.

Ventricular Couplets (V-Couplet) – two ventricular premature complexes in a row

Ventricular Triplets (V-Triplet) – three ventricular premature complexes in a row

Ventricular Tachycardia (VT) – more than three consecutive VPCs at a rate  $\geq$  to the surrounding sinus complexes.

Atrial Premature Complexes (APC) – a normally conducted sinus complex with RR interval of  $<45\%$  of the preceding RR interval. A p wave may be identifiable for these complexes and may be of similar or differing morphology or hidden within the preceding T wave. These complexes appear nearly identical in morphology to the surrounding normal sinus complexes.

Supraventricular Tachycardia (SVT) – more than three consecutive APCs at a rate  $\geq$  to the surrounding sinus complexes.

Supraventricular Couplet (SV-Couplet) – two supraventricular premature complexes in a row

Supraventricular Triplet (SV-Triplet) – three supraventricular premature complexes in a row

Ventricular Bigeminy –  $> 2$  cycles of alternating sinus complexes and ventricular premature complexes.

Ventricular Trigeminy –  $> 2$  cycles of alternating 2 sinus complexes and ventricular premature complexes.

Supraventricular Bigeminy (SV-Bigeminy) –  $> 2$  cycles of alternating sinus complexes and supraventricular premature complexes.

Supraventricular Trigeminy (SV-Trigeminy) –  $> 2$  cycles of alternating 2 sinus complexes and supraventricular premature complexes.

Second Degree Atrioventricular Block (2-AVB) – defined as the presence of  $\leq 2$  non-conducted p waves in a row observed on the ECG tracing. Mobitz type I or II was not determined.

High-grade Second Degree Atrioventricular Block (HG2-AVB) – defined as the presence of  $\geq 3$  non-conducted p waves in a row observed on the ECG tracing.

Complete Atrioventricular Block (3-AVB) – defined as a period with continuous non-conducted p waves and a compensatory ventricular escape rhythm.

Ventricular Escape Rhythm – A ventricular ectopic event meeting the same wide and bizarre criteria as VPC but lacking the previously noted prematurity. These beats may occur as single ectopic foci or as a repeating rhythm in the case of complete AV block.

Sinus Arrhythmia – A rhythm where the complexes are of sinus origin yet the R-R intervals are irregular (this does not include irregularities caused by AV block events or ectopy).

**Severity of Arrhythmia Scoring Scheme.** Numeric (continuous) and categorical scoring schemes were evaluated for interpreting the severity of cardiac arrhythmias within supraventricular ectopy, ventricular ectopy and atrioventricular block categories. Additionally, an overall arrhythmia severity score which encompasses supraventricular ectopy, ventricular ectopy and atrioventricular block was evaluated.

*Severity of Ventricular Ectopy.*

Method 1: Numeric Assessment

The total number of ventricular ectopic events was compared by strain and treatment group.

Method 2: Categorical Severity Assessment

A modification of the Lown Ventricular Arrhythmia Severity Score was utilized (Lown et al., 1975). The arrhythmias were graded as category 0 – 5. The highest category observed on a single recording is the grade assigned to the sample.

Category 0 – No observed ventricular ectopy.

Category 1 – Occasional (<50 during recording period) single VPCs

Category 2 – Frequent single VPCs (>50 during recording period)

Category 3 – Multiform /Polymorphic VPBs and/or Ventricular Couplets

Category 4 – Repetitive VPC (V-triplets, bigeminy, trigeminy)

Category 5 – Paroxysms of Ventricular Tachycardia / RonT Phenomenon

*Severity of Supraventricular Ectopy.*

Method 1: Numeric Assessment

The total number of supraventricular ectopic events was compared by strain and treatment group.

Method 2: Categorical Assessment

Categorical severity assessment was performed where grade 1 represented single supraventricular premature complexes and grade 2 represented repetitive APC morphologies. The highest category observed on a single recording is the grade assigned to the sample.

Category 0 – No observed supraventricular ectopy

Category 1 – Single APCs observed

Category 2 – Repetitive APCs observed (SV-couplets, SV-triplets, SV-bigeminy, SV-trigeminy, SVT)

*Severity of Atrioventricular Block.*

Method 1: Numeric Assessment

The total number of atrioventricular block events (blocked p-waves) was compared by strain and treatment group.

Method 2: Categorical Assessment Categorical severity assessment was performed where grade 1 represented second-degree AV Block; Grade 2 represented high-grade second-degree AV block and grade 3 represented paroxysmal complete AV block. The highest category observed on a single recording is the grade assigned to the sample.

Category 0 – No observed AVB

Category 1 – 2-AVB observed

Category 2 – HG2-AVB observed

Category 3 – 3-AVB observed

*Overall Arrhythmia Severity Score.* The overall arrhythmia severity score represents the sum of categorical assessments for all prior categories. The categorical severity assigned for

ventricular ectopy, supraventricular ectopy and atrioventricular block events was totaled. The maximum total score is 10 while the minimum is 0.

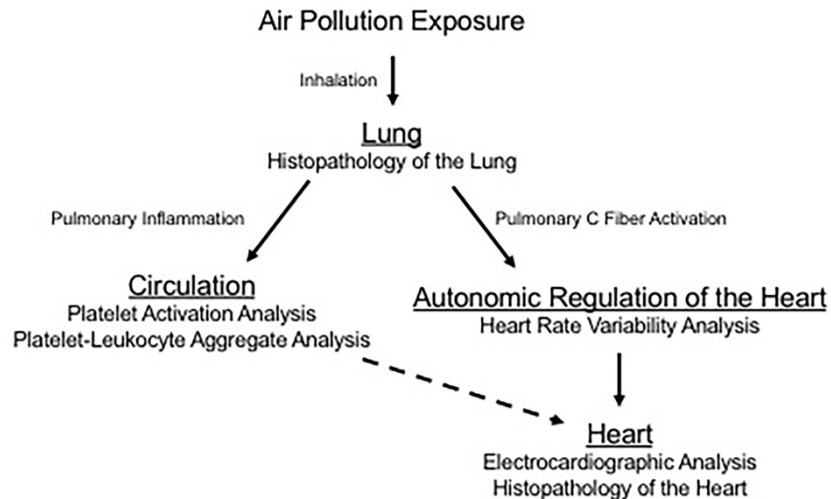
**Statistical Analysis.** Data was tested for normality with a D'Agostino & Pearson normality test prior to evaluation of differences by exposure group. Normal distributed data was evaluated with a One-way ANOVA followed by a Tukey's test of multiple comparisons. Non-parametric data was evaluated with a Kruskal-Wallis test followed by a Dunn's test of multiple comparisons. Alpha was set at a  $P < 0.05$ . Differences by strain were visually inspected and not tested given the large degree of overlap as evidenced by the provided graphs. Graphed data shows median and interquartile range for each exposure group. Brackets signify significant differences between the groups after correction for multiple comparisons. All statistical evaluation and provided graphs were generated by Graphpad Prism 7 for Mac.

#### **H. Statistical Analysis:**

All data were examined for normality by D'Agostino & Pearson normality test. Non-normally distributed data (lung and heart pathology; arrhythmias) were analyzed by Mann-Whitney U (t-test) and Kruskal-Wallis test for multiple comparisons. Normally distributed data (white blood cell and platelet parameters, HRV measures) were analyzed by Wilcoxon tests (for t-test), ANOVA (for multiple comparisons) or for data containing within animal HRV time- and frequency-domain data by mixed model two-way analysis of variance (ANOVA) with repeated measures (IBM SPSS Software; IBM Analytics, Armonk, New York)(Littell et al., 1998). There are two steps in performing a mixed model two-way ANOVA with repeated measures (Littell et al., 1998). In the first step, the best fit of the data to one of several within-subject covariance structures is determined using the Akaike information criterion (AIC) and the Schwarz Bayesian criterion (SBC). In the second step we analyzed the strain, time and protocol effects by estimating and comparing means, using a Bonferroni adjustment (IBM Institute). Having analyzed the data in a manner that allowed for the evaluation of the time and exposure effects by rat strain, we reanalyzed the data, focusing on the effect that each protocol had on HRV measures compared to the baseline values. An alpha-priori of  $< 0.05$  were considered statistically significant.

## RESULTS:

We examined the biological effects of exposure to identify potential pathways linking air pollution exposure to cardiac events, results are presented in the order illustrated in the diagram below. Briefly, the effects of air pollution are instigated in the lung through inhalation, activating pulmonary C fibers as well as damaging the pulmonary epithelium, which promotes inflammation. Pulmonary inflammation promotes platelet activation and platelet-leukocyte interactions, which can lead to microthrombi formation in systemic circulation (2). Pulmonary C fiber activation alters autonomic balance, and thus, autonomic regulation of heart rate, causing decreases in heart rate variability (3), and increasing the appearance of arrhythmias (4). Ultimately, these changes increase the potential for cardiac event occurrence (5).



### Histopathology of the Lung:

*Age-Related Lung Lesions.* Terminal bronchiolar regions of FA-exposed NW and SH rats were similar and commonly displayed cuboidal bronchiolar epithelium and alveolar ducts lined by thin alveolar walls overlain by squamous type I pneumocytes, consistent with examples from studies using juvenile rats (Figure 1A,B). Some age-related lesions were evident in both NW and SH rats. The most frequent change was focal, often subpleural, accumulations of large foamy macrophages. In addition, rats occasionally had small foreign body granulomas.

*UFPM-Induced Airway Lesions.* Rats exposed to UFPM had only minimal lesions throughout the lung (Figure 2A,B).

*O<sub>3</sub>-Induced Airway Lesions.* Rats exposed to O<sub>3</sub> had lesions predominately in the terminal bronchioles and alveolar ducts (Figure 1C,D), however, injury extended into the large airways of SH rats (Figure 3A). Terminal bronchioles of O<sub>3</sub>-exposed NW rats were hyperplastic and walls were thickened by edema and cellular infiltrates (Figure 1C). Alveolar duct walls were more prominent due to interstitial edema and modest cellularity. Some lesions presented alveoli containing proteinaceous exudate. The large airways of O<sub>3</sub>-exposed NW rats did not differ from FA or UFPM-exposed NW rats.

In SH rats, the terminal bronchioles had intraluminal proteinaceous and cellular exudate, attenuated epithelium, mural edema and inflammatory cell infiltrate (Figure 1D). Alveolar ducts were thickened by interstitial edema and lumens contained proteinaceous exudate. The large airways of O<sub>3</sub>-exposed SH rats displayed attenuated epithelium, sloughed epithelial cells and intramural PMN's (Figure 3A).

*Combined-Pollutant Exposure Induced Airway Injury.* Overall the most severe and generalized lesions were present in rats exposed to UFPM+O<sub>3</sub> (Figure 2C,D and 3B). Terminal bronchiolar epithelium was degenerate or necrotic with luminal debris admixed with neutrophils. Terminal bronchiolar walls were expanded by edema in the adventitial sheath and contained

extravascular and transmigrating neutrophils. Pulmonary arterioles at the terminal bronchiolar junction also had edematous adventitia and prominent endothelium often overlain by marginated neutrophils. Alveoli along the alveolar duct contained moderate numbers of neutrophils and occasional macrophages. In more severe lesions the alveolar duct and adjacent parenchymal alveoli contained wispy proteinaceous exudate admixed with occasional sloughed squamous epithelial cells. Some capillaries in alveolar ducts were distended by microthrombi. Luminal exudates of PMNs and necrotic epithelial cell debris were more prominent in SH as compared with NW rats.

The bronchi of UFPM+O<sub>3</sub>-exposed rats of both strains had ciliary cell loss and necrosis of airway epithelium with accumulations of cellular debris lining the airway surface (Figure 3B). Some airways were lined by attenuated squamous epithelial cells and others had evident transmigrating neutrophils.

*Impact of Age and Surgical Procedures.* To determine the impact of time (days) between telemeter implantation and exposure as well as age (wks) at exposure on pathological changes in the lung, a two-way analysis of variance with Bonferroni post-hoc comparisons was used to identify significant differences between strains and exposure groups with time between telemeter implantation and exposure as well as age at exposure as covariate factors. There were no significant effects with either time between telemeter implantation and exposure ( $21.2 \pm 1.4$  days) or age at exposure ( $45.1$  wks  $\pm 6$  days) between strains or exposure group.

Table I. Histopathologic measures of the lung in normal and spontaneously hypertensive rats following exposure (mean  $\pm$  SEM).

Parameter	NW				SH			
	FA (n = 10)	UFPM (n = 8)	O <sub>3</sub> (n = 9)	UFPM+O <sub>3</sub> (n = 11)	FA (n = 12)	UFPM (n = 10)	O <sub>3</sub> (n = 8)	UFPM+O <sub>3</sub> (n = 12)
Macrophage Infiltrate	0.5 $\pm$ 0.2	0.8 $\pm$ 0.2	1.3 $\pm$ 0.3	2.8 $\pm$ 0.2 <sup>*,**,#</sup>	0.2 $\pm$ 0.1	0.6 $\pm$ 0.3	0.8 $\pm$ 0.2	2.6 $\pm$ 0.2 <sup>*,**,#</sup>
Edema	0.4 $\pm$ 0.2	0.3 $\pm$ 0.1	0.9 $\pm$ 0.3	3.7 $\pm$ 0.1 <sup>*,**,#</sup>	0.2 $\pm$ 0.1	0.0	2.3 $\pm$ 0.4 <sup>*,**,##</sup>	3.5 $\pm$ 0.3 <sup>**,</sup>
PMN Infiltrate	0.6 $\pm$ 0.2	0.1 $\pm$ 0.1	1.0 $\pm$ 0.4	3.8 $\pm$ 0.1 <sup>*,**,#</sup>	0.3 $\pm$ 0.2	0.4 $\pm$ 0.3	2.4 $\pm$ 0.3 <sup>*,##</sup>	4.0 $\pm$ 0.2 <sup>**,</sup>
TB Epithelial Necrosis	0.0	0.0	0.4 $\pm$ 0.3	3.8 $\pm$ 0.1 <sup>*,**,#</sup>	0.1 $\pm$ 0.1	0.0	2.2 $\pm$ 0.3 <sup>*,**,##</sup>	3.7 $\pm$ 0.2 <sup>**,</sup>
Exudate	0.0	0.0	0.3 $\pm$ 0.2	3.7 $\pm$ 0.2 <sup>*,**,#</sup>	0.0	0.1 $\pm$ 0.1	1.2 $\pm$ 0.3 <sup>##</sup>	3.5 $\pm$ 0.3 <sup>**,</sup>
LA Cilia Cell Loss/Necrosis	0.8 $\pm$ 0.2	0.0	0.2 $\pm$ 0.1	3.8 $\pm$ 0.2 <sup>*,**,#</sup>	0.1 $\pm$ 0.1	0.0	1.3 $\pm$ 0.3 <sup>*,**,#</sup>	3.1 $\pm$ 0.3 <sup>**,</sup>
IVFNA	0.0	0.8 $\pm$ 0.4	0.9 $\pm$ 0.5	0.8 $\pm$ 0.2	0.6 $\pm$ 0.2	1.9 $\pm$ 0.4 <sup>*</sup>	1.9 $\pm$ 0.5	1.3 $\pm$ 0.2
Intravenous Thrombus	0.0	1.8 $\pm$ 0.4	0.8 $\pm$ 0.4 <sup>*</sup>	1.3 $\pm$ 0.4	0.4 $\pm$ 0.2	1.0 $\pm$ 0.4	0.4 $\pm$ 0.3	0.9 $\pm$ 0.3

Note: Standard, paraffin-embedded, histopathologic sections of lung tissue were evaluated by a board-certified veterinary pathologist for lesions in the large airways, terminal bronchiolar/alveolar duct regions, alveolar parenchyma and vasculature and assigned a severity score (0-5). Note: Normal Wistar rat (NW); Spontaneously Hypertensive rat (SH); filtered air (FA); ultrafine particulate matter (UFPM); ozone (O<sub>3</sub>); ultrafine particulate matter combined with ozone (UFPM+O<sub>3</sub>); polymorphonuclear leukocyte (PMN); terminal bronchiole (TB); large airway (LA); intravenous fibrin-neutrophil aggregates (IVFNA); the Kruskal-Wallis test was used to calculate the difference between exposure groups by strain and significant *p*-values (*p* < 0.05) from Dunn-Bonferroni post-hoc test are shown in table. Values are shown as the means  $\pm$  SEM by exposure group and strain.

\* Significant compared to FA within same strain exposure groups.

\*\* Significant compared to UFPM within same strain exposure groups.

# Significant compared to O<sub>3</sub> within same strain exposure groups.

## Significant difference between NW and SH within same strain exposure groups.

Figure 1:

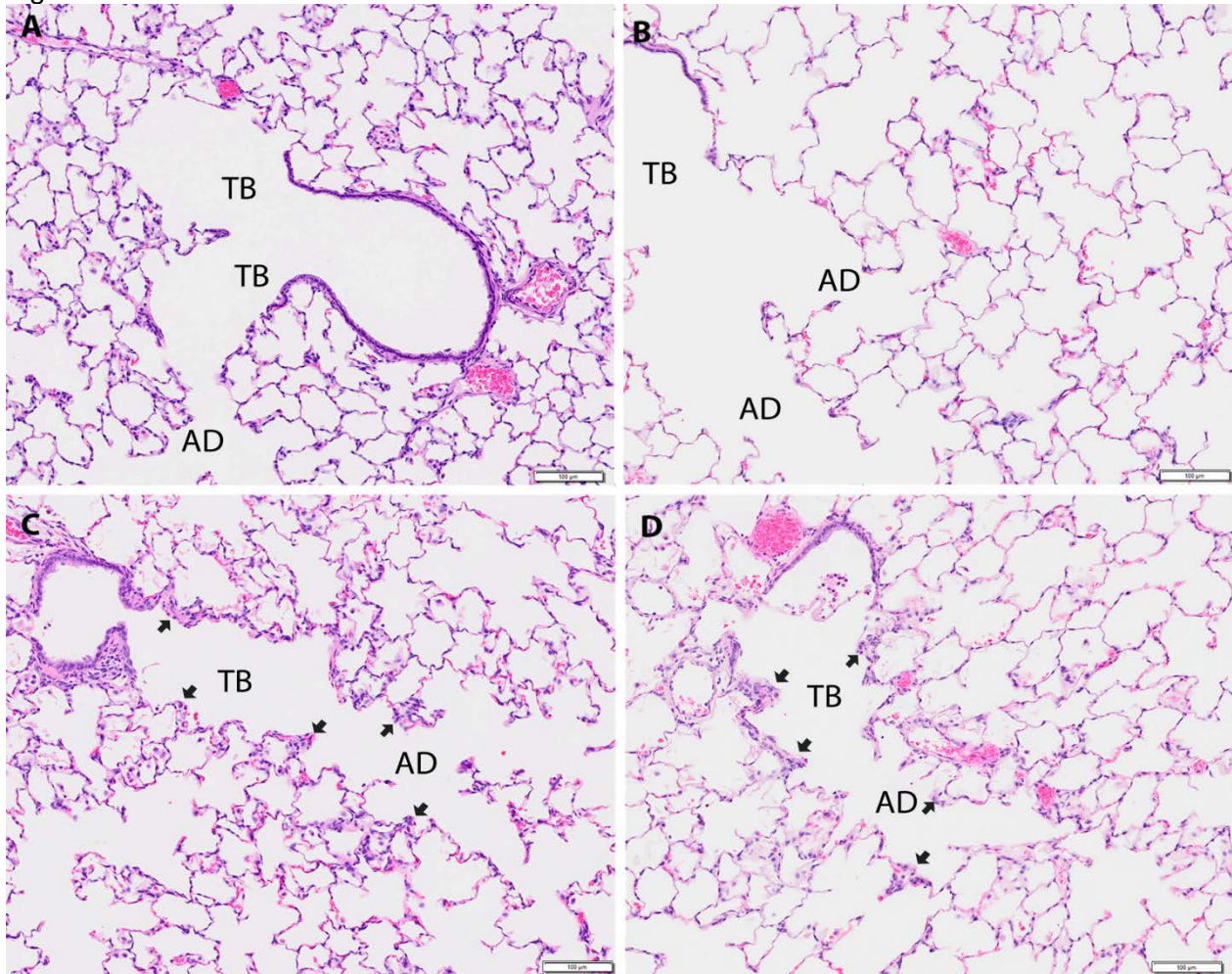


Figure 1. Terminal bronchioles and alveolar ducts from NW and SH rats by experimental exposure. (A) FA NW rat terminal bronchioles have cuboidal bronchiolar epithelium and alveolar ducts lined by thin alveolar walls overlain by squamous type I pneumocytes. (B) FA SH rat terminal bronchioles are identical to NW rat. (C) O<sub>3</sub> NW rat terminal bronchioles have hyperplastic epithelium and walls thickened by edema and cellular infiltrates. Alveolar duct walls are more prominent due to interstitial edema and modest cellularity. Some alveoli contain proteinaceous exudate. (D) O<sub>3</sub> SH rat terminal bronchiole with intraluminal proteinaceous and cellular exudate, attenuated epithelium suggestive of previous necrosis and migratory repair, mural edema and inflammatory cell infiltrate. Alveolar ducts are thickened by interstitial edema and lumens contain proteinaceous exudate.

Figure 2:

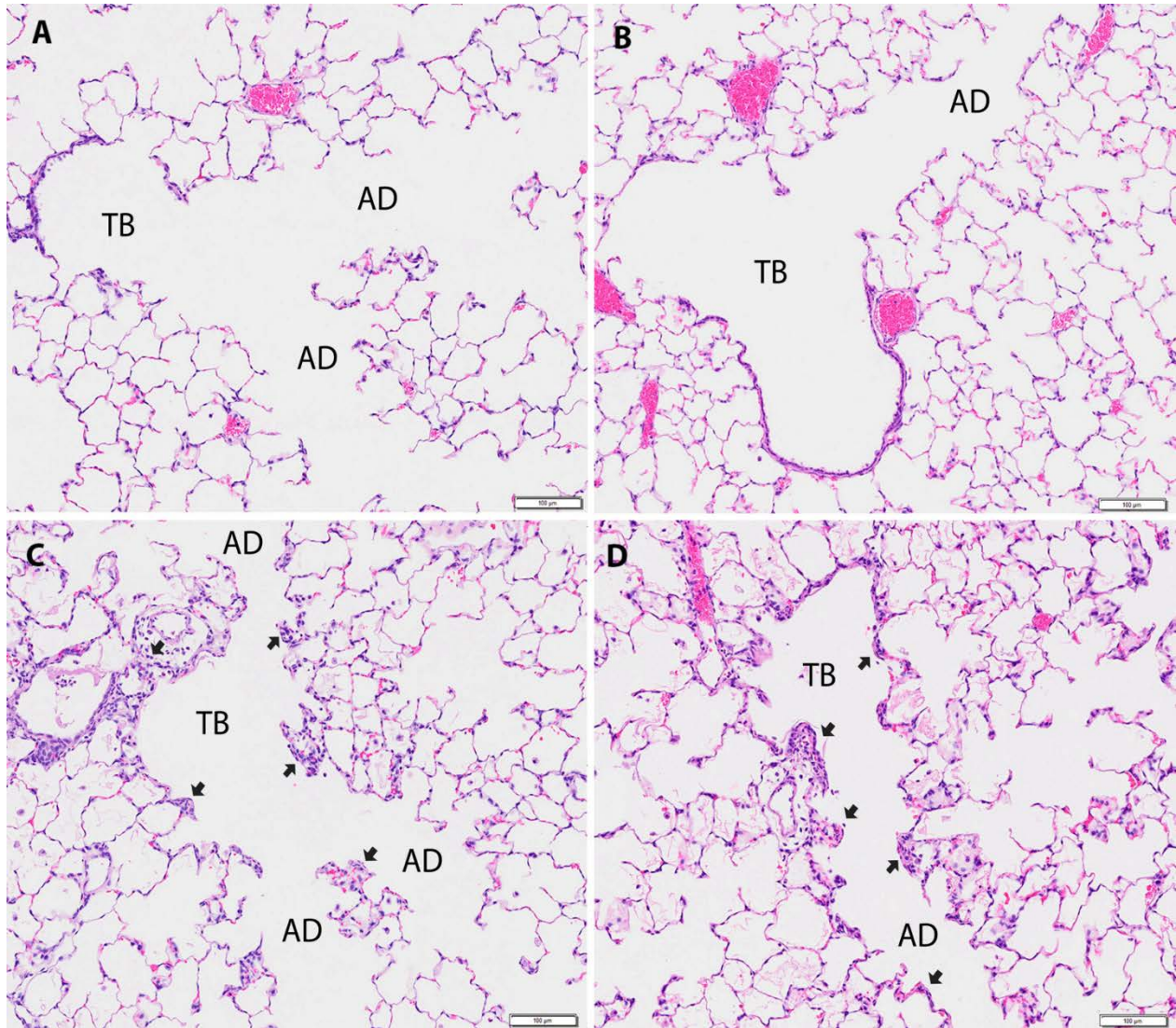


Figure 2. Terminal Bronchioles and alveolar ducts from UFPM or UFPM+O<sub>3</sub>-exposed NW and SH rats. A) UFPM-exposed NW rat terminal bronchiole did not differ from FA controls. B) UFPM-exposed SH rat terminal bronchiole did not differ from FA controls. C) Terminal bronchiole from a NW rat exposed to UFPM+O<sub>3</sub> shows epithelial necrosis, luminal exudate and extensive mural edema with inflammatory cell accumulation. Note inflammatory cell accumulation in arteriolar adventitia. D) Terminal bronchiole from a SH rat exposed to UFPM+O<sub>3</sub> shows similar epithelial loss and inflammation. Desquamate type I pneumocytes are evident in alveolar duct and surrounding alveoli where they are admixed with proteinaceous exudate.

Figure 3:

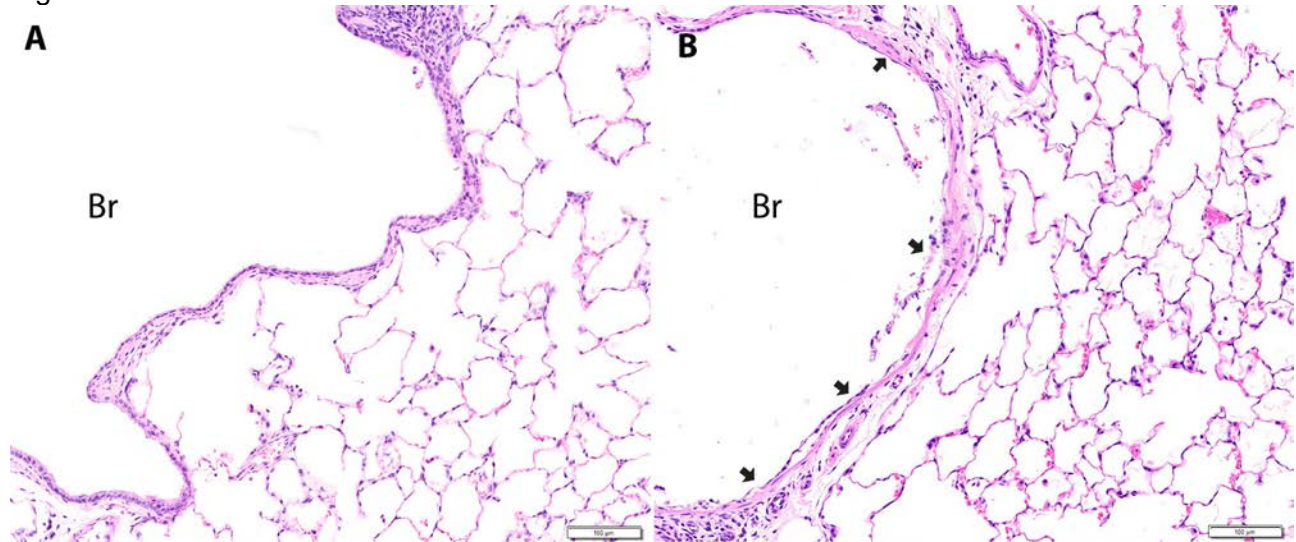


Figure 3. Large airways from O<sub>3</sub> or UFPM+O<sub>3</sub> exposed SHR rat. A) Large airway from O<sub>3</sub> exposed SHR rat does not differ from filtered air or UFPM exposed animals of either strain. B) Large airway from UFPM+O<sub>3</sub> exposed SHR rat has sloughed epithelial cells and mural edema. Some airway surface lacks epithelial lining while other regions are lined by attenuated squamous epithelial cells.

### **Hematology / Flow Cytometry:**

Note that blood samples taken at baseline were obtained from the tail vein (small vessel with high shear) of anesthetized rats, while those taken at necropsy were taken from the vena cava (large vessel with low shear). Blood cells in general move in differing patterns in small vs large vessels –such that the number of any given cell type (which may not truly vary) may be different when taken in small vs large vessels. In addition, baseline samples were obtained over the course of more than a year, and necropsy samples were obtained often several months after baseline samples.

### **Platelet Counts** ( $\times 10^6$ /ul) mean +/-SEM:

By Strain:

**NW rats:** There were no significant differences between exposure conditions.

**SH Rats:** There were no differences in the platelet concentrations between exposure conditions.

**Strain Differences:** When comparing the difference between the strains at baseline there was a statistically significant difference between the total numbers of platelets within each strain  $p=0.0101$ . The mean of the SH rats was  $500.3 \pm 25.43 \times 10^6$ /ul, while that of the NW was  $590.5 \pm 22.04 \times 10^6$ /ul.

### **White Blood Cell (WBC) Counts**(/ul):

**NW Rats:** There was a statistically significant difference between FA ( $12056 \pm 1721$ ) and UFPM+O<sub>3</sub> ( $5509 \pm 539.8$ )  $p=0.0059$ .

**SH Rats:** There was a significant difference in the total WBC counts between FA ( $9138 \pm 889.9$ ) and UFPM+O<sub>3</sub> ( $4555 \pm 713.7$ ) ( $p=0.0006$ ) in the exposure samples.

**Strain Differences:** Comparison of baseline WBC counts demonstrated that there was strain to strain variation that was statistically significant. Overall SH rats had a lower total white cell count ( $5,129 \pm 197.7$ ) than Normal Wistar rats ( $6,350 \pm 274.2$ ) with a  $p$  value =0.0005.

**Flow Cytometry Data Analysis:** All staining was done on platelets which were not permeabilized, and thus only the proteins expressed on the platelet surface were studied. The following proteins were examined:

- CD61 is constitutively expressed on the platelet surface, but with platelet activation the number of the integrins can either increase, as the result of alpha granule secretion, as they are also on the alpha granule membrane; or it can decrease which can be due either to endocytosis and recycling or being budded off into microvesicles.
- CD62P (P-selectin) is an alpha granule membrane protein which is expressed on the platelet surface when platelet alpha granules are secreted and platelets are activated.
- CD63 is a lysosomal granule membrane protein, which, similar to P-selectin is only expressed on the platelet surface when platelets are activated and have secreted their lysosomal granules.
- CD11b (integrin  $\alpha$ M) is constitutively expressed on the neutrophil surface
- CD18 (integrin  $\beta$ 2) is constitutively expressed on the surface of all leukocytes
- CD61/11b is a population of platelet/neutrophil aggregates
- CD61/18 is a population positive for both platelets and leukocytes
- White cell populations (CD11b, CD18 as well as CD61/11b and CD61/18) were based on log-log data analysis of forward (FS) and side scatter (SS) of the large (FS) and granular (SS) population. CD61 positive events (in the absence of CD11b or CD18) are indicative of platelet aggregates based on forward and side scatter.

For each of the markers (CD61,62P, CD63, CD11b, CD18, CD61/11b and CD61/18) flow analysis provides information on the percent positive cells as well as the mean fluorescence intensity (MFI) of the positive population. Percent positive cells are the percent of cells (per 10,000 platelets or white blood cells) that express the receptor/protein of interest. Mean fluorescence intensity is a relative measure (arbitrary fluorescent units – AFU) of the numbers of molecules of interest present on the cell surface.

Note: Blood samples for flow cytometry taken at baseline were obtained from the tail vein (small vessel with high shear) of anesthetized rats, while those taken at necropsy were taken from the vena cava (large vessel with low shear). In addition, baseline samples were obtained over the course of more than a year, and necropsy samples were obtained often several months after baseline samples. Further, platelets can be activated by shear in small vessels, thus it is very difficult to compare platelet activation between baseline with exposure conditions. This is also true for platelet aggregates and platelet-white cell aggregates. It is, however, useful to compare baseline data between the two different strains of rats.

#### **Platelet Flow Data:**

##### ***Percent Positive (%+) Platelets***

##### ***NW rat platelets:***

*Exposure:* There were no significant differences in the %+ of CD61, 62P or 63 in the exposure conditions.

##### ***SH rat platelets:***

*Exposure:* With regard to the % positive platelets of SH rats – there were no differences in any of the three markers between exposures.

##### ***Mean Fluorescence Intensity (MFI (AFU)):***

##### ***NW rat platelets:***

*Exposure:* There was a significant difference for CD 61 mean MFI between O<sub>3</sub>(40119+/-3119) and UFPM (51418+/-1311) p=0.0383. There were no significant differences in either CD62P or CD63 between the different exposure groups.

##### ***SH rat platelets:***

*Exposure:* There were no significant differences in the mean MFI of either CD62P or CD63 between any of the exposure conditions. However, comparing the conditions for CD61 there were significant differences between the means of FA (4264+/-2711) and UFPM+O<sub>3</sub> (53704+/-1165) p=0.0123; between O<sub>3</sub> (36343+/-4681) and UFPM+O<sub>3</sub> (53704+/-1165) p=0.0046; and between O<sub>3</sub> (36343+/-4681) and UFPM (52472+/-1374) p=0.0234.

##### ***Strain Differences:***

There was a statistically significant difference in the CD61%+ between the NW (78.02+/-1.495) and SH (60.13+/-3.55) rats p=0.0002. There was no significant difference in the CD62P, no in the CD63 %+ platelets between the strains. There was no significant difference in the CD61MFI, CD62P MFI or CD63 MFI between the strains.

##### **MICROVESICLES: CD61%+ and MF:**

Platelet microvesicles are defined as CD61+ vesicles based on forward scatter with the x-axis threshold set at 10<sup>1</sup> and the use of fluorescent beads of defined size.

##### ***NW rat platelet microvesicles:***

%+CD61: There were significant differences in CD61 %+ exposure samples between O<sub>3</sub> (26.4) and UFPM+O<sub>3</sub>(13.75) p=0.0224

CD61 MFI: In exposure conditions, there were no significant differences in the mean MFI of CD61+ platelets for any conditions.

### ***SH rat platelet microvesicles:***

%+CD61: There were significant differences in the %CD61 positive in the exposure conditions between O<sub>3</sub> (30.5%) and UFPM (13.9%) p= 0.0165 as well as O<sub>3</sub> (30.5%) and the combined pollutants (13.64%) p=0.0123.

CD61 MFI There were no significant differences in the MFI of CD61 between any of the exposure conditions.

### **White Blood Cell (WBC), Platelet Aggregate and WBC-Platelet Aggregate Data:**

#### **By Strain:**

#### **Normal Wistar:**

#### **Percent Positive Cells:**

*Between exposure conditions:* There were significant differences between FA (23.31) and UFPM (10.71) for **61/11b** p=0.0445. There also were significant differences in %+ **CD11b** between mean of FA (23.81) and UFPM+O<sub>3</sub> (12.55) p=0.0459. However, there were no significant differences for CD61/18, CD61, CD18 between any of the condition.

#### **Mean Fluorescence Intensity (MFI AFU):**

*Between exposure conditions:* There were no significant differences between the MFI of any of the variables (CD61, CD11b or CD18) between the conditions.

#### **Spontaneously Hypertensive Rats:**

#### **Percent Positive Cells:**

*Between Exposure conditions:*

**CD61:** There were significant differences between FA (65.21) and UFPM (28.46) p=0.0175; as well as between FA (65.21) and UFPM+O<sub>3</sub> (23.6) p=0.0019. Additionally, there were significant differences between O<sub>3</sub> (70.01) and UFPM (28.46) p=0.0074 as well as between O<sub>3</sub> (70.01) and UFPM+O<sub>3</sub> (23.6) p=0.0007. **CD11b:** There was a significant difference between FA (20.54+/-2.758) and UFPM+O<sub>3</sub> (5.559+/-1.587) p=0.0121.

**CD18:** There also was a significant difference between the means of O<sub>3</sub> (27.22+/-9.557) and UFPM+O<sub>3</sub> (5.521+/-1.46) p=0.0165, as well as between FA (24.28+/-5.052) and UFPM+O<sub>3</sub> (5.521+/-1.46) p=0.0058.

**CD11b/61:** When examining the aggregates of platelets and white cells there were significant differences between all of the exposures p=0.0255.

**CD18/61:** Similarly, to the CD11b/61, when examining the CD18/61 aggregate the only difference in %+ CD18/CD61 was between O<sub>3</sub> (22.54+/-9.124) and UFPM+O<sub>3</sub> (4.626+/-1.419) p=0.0410.

#### **Mean Fluorescence Intensity (MFI)**

*Between exposure conditions:*

There were no statistically significant differences for CD61 between any of the 4 exposure conditions.

The only difference in CD11b MFI was between FA (24.33) and UFPM+O<sub>3</sub> (9.889) p=0.0114.

The only significant difference in CD18 MFI was between FA (24.89) and UFPM+O<sub>3</sub> (11.06) p=0.0402.

**Rat Strain Differences:**

Baseline CD11b: There was a statistically significant difference between the CD11b %+ for the NW (mean rank=24.93) and the SH rats (mean rank = 38.74); reflecting a greater degree of inflammation in the SH rats at baseline ( $p=0.004$ ).

Baseline CD61/CD11b (platelet/WBC aggregates): There were statistically significant differences between CD61/CD11b %+ aggregates; the mean rank of NW = 23.91 while that of SH rats = 39.46 ( $p=0.001$ ), another measure of inflammation.

Figure 4:

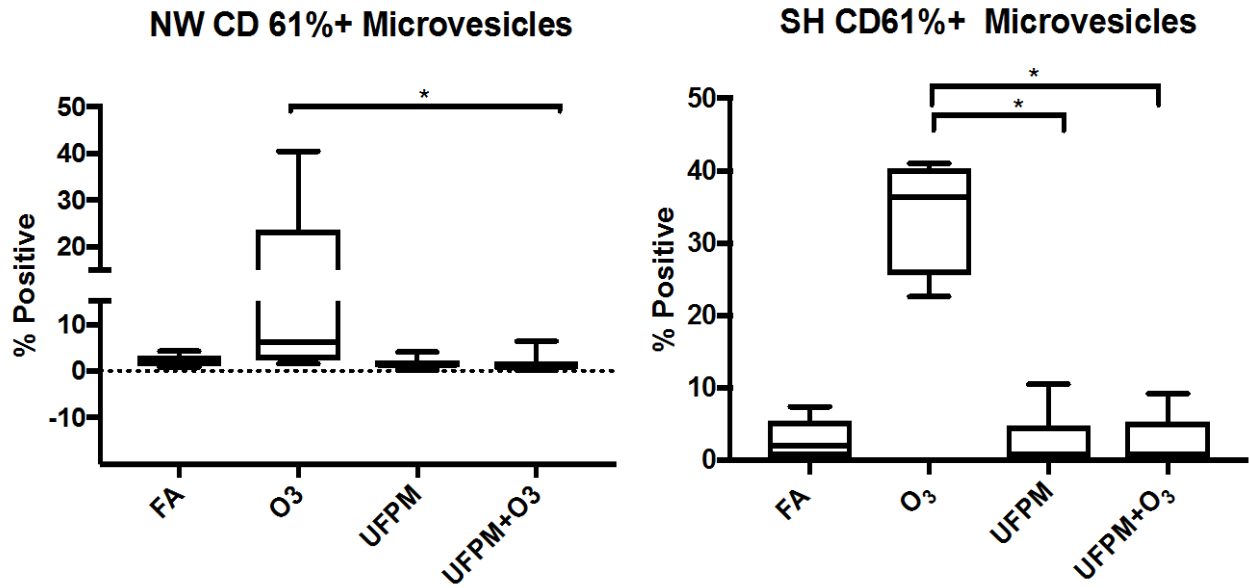
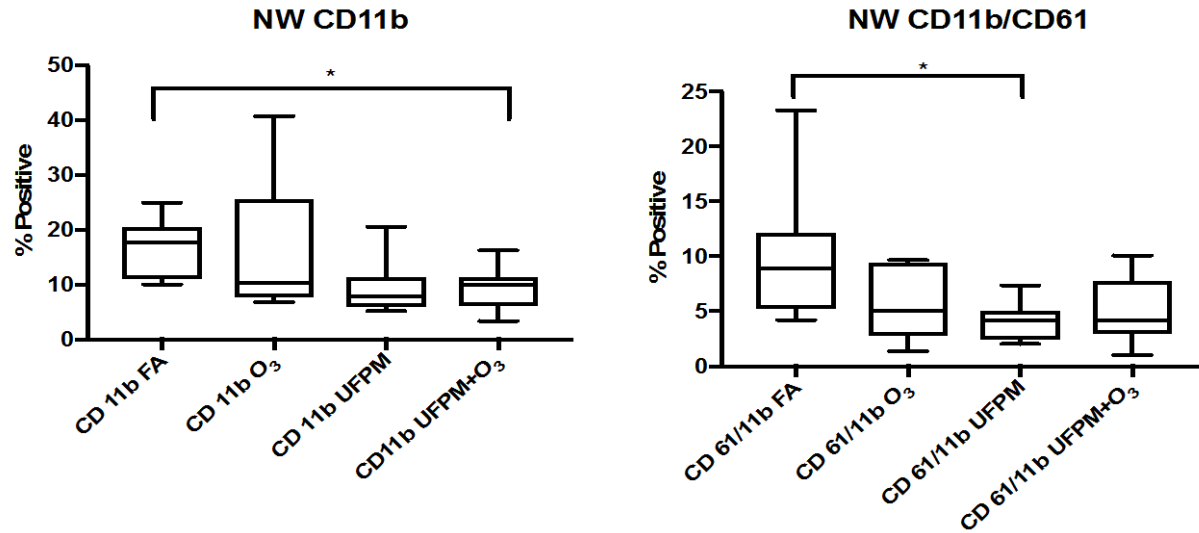


Figure 4. Both NW and SH rats had significant differences in the percent CD61+ microvesicles between ozone exposures and combined pollutants. However, there were also significant differences between ozone and UFPM CD61+ microvesicles in the SH rat population. \*= $p \leq 0.05$ .

Figure 5:



A.

B.

Figure 5. NW Rats only showed differences in the number of positive cells for CD11b. Within that group, there was only a statistical difference between animals exposed to FA and those exposed to the combined pollutants, there was only a difference between FA and UFPM. \*= $p \leq 0.05$ ; \*\*= $p \leq 0.01$

Figure 6:

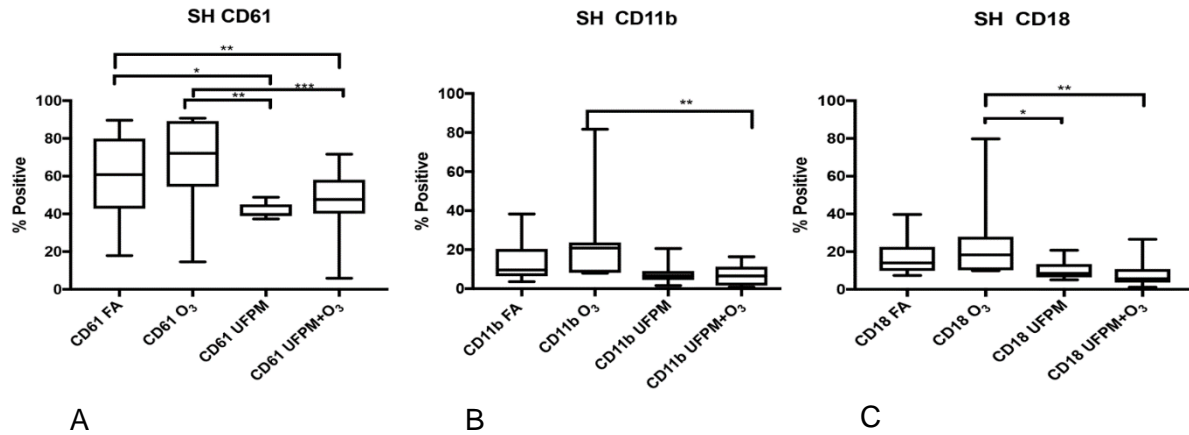


Figure 6. SH rats showed significant inflammatory changes in the peripheral blood, as reflected by changes in the percent of CD61 positive cells reflective of platelet aggregates (A), CD11b (B) and CD18 (C) in combined pollutants. In addition, there are significant decreases in between ozone and UFPM both for CD61 as well as CD18. As described in the lung pathology section, this is in keeping with increased microthrombi in the terminal bronchiolar aspects of the lung. \*= $p \leq 0.05$ ; \*\*= $p \leq 0.01$

Table II. Platelet and White Blood Cell (ul) Counts (means  $\pm$  SEM).

Parameter	FA	UFPM	O3	UFPM+O3	FA	UFPM	O3	UFPM+O3
Blood Counts								
Platelets ( $\times 10^9/\mu\text{l}$ )	798.3 $\pm$ 59.55	835.0 $\pm$ 57.97	653.1 $\pm$ 56.32	694.5 $\pm$ 22.36	591.8 $\pm$ 58.5	633.1 $\pm$ 42.45	549.5 $\pm$ 62.9	692.3 $\pm$ 25.48
WBC ( $\mu\text{l}$ )	12056 $\pm$ 1721	6314 $\pm$ 786	7400 $\pm$ 986.3	5509 $\pm$ 539.8	9138 $\pm$ 889.9	6563 $\pm$ 603.8	6389 $\pm$ 807.2	4555 $\pm$ 713.7

Normal Wistar rat (NW); Spontaneously Hypertensive rat (SH); filtered air (FA); ultrafine particulate matter (UFPM); ozone ( $O_3$ ); ultrafine particulate matter combined with ozone (UFPM+ $O_3$ ); white blood cell (WBC); the Kruskal-Wallis test was used to calculate the differences between exposure groups by strain and significant  $p$ -values ( $p < 0.05$ ) from Dunn-Bonferroni post-hoc test are shown in table. Values are shown as the means  $\pm$  SEM by exposure group and strain.

\* Significant compared to FA within same strain exposure groups.

\*\* Significant compared to UFPM within same strain exposure groups.

# Significant compared to  $O_3$  within same strain exposure groups.

Table III. Platelet Flow Cytometry Percent-Positive and Mean Fluorescence Intensity (means  $\pm$  SEM).

Parameter	NW				SH			
	FA	UFPM	O <sub>3</sub>	UFPM+O <sub>3</sub>	FA	UFPM	O <sub>3</sub>	UFPM+O <sub>3</sub>
Platelet Markers								
CD61 %+	82 $\pm$ 2.385	79.73 $\pm$ 1.667	76.8 $\pm$ 5.565	74.79 $\pm$ 2.71	63.43 $\pm$ 5.26	65.74 $\pm$ 7.18	63.58 $\pm$ 9.19	49.37 $\pm$ 7.29
CD62 %+	15.71 $\pm$ 6.642	18.42 $\pm$ 6.264	22.89 $\pm$ 9.183	16.13 $\pm$ 3.495	20.72 $\pm$ 3.82	13.28 $\pm$ 3.91	9.868 $\pm$ 3.25	7.126 $\pm$ 1.07
CD63 %+	11.94 $\pm$ 4.824	6.123 $\pm$ 1.063	10.02 $\pm$ 2.455	6035 $\pm$ 0.71	9.767 $\pm$ 2.26	7.855 $\pm$ 1.34	15.96 $\pm$ 8.02	11.2 $\pm$ 1.435
CD61 MFI	42689 $\pm$ 2912	51418 $\pm$ 1311	40119 $\pm$ 3119	48699 $\pm$ 2310	42641 $\pm$ 2711	52472 $\pm$ 1374	36353 $\pm$ 4681	53704 $\pm$ 1165
CD62 MFI	7164 $\pm$ 4005	1431 $\pm$ 336.8	9787 $\pm$ 8929	1366 $\pm$ 328.5	85727 $\pm$ 83169	2517 $\pm$ 990.0	3089 $\pm$ 1830	2256 $\pm$ 827.3
CD63 MFI	39403 $\pm$ 15425	230655 $\pm$ 138394	385308 $\pm$ 223555	45531 $\pm$ 18996	157230 $\pm$ 75688	108626 $\pm$ 79495	145722 $\pm$ 110252	181679 $\pm$ 109501

Normal Wistar rat (NW); Spontaneously Hypertensive rat (SH); filtered air (FA); ultrafine particulate matter (UFPM); ozone (O<sub>3</sub>); ultrafine particulate matter combined with ozone (UFPM+O<sub>3</sub>); percent-positive (%+); mean fluorescence intensity (MFI); the Kruskal-Wallis test was used to calculate the difference between exposure groups by strain and significant *p*-values (*p* < 0.05) from Dunn-Bonferroni post-hoc test are shown in table. Values are shown as the means  $\pm$  SEM by exposure group and strain.

\* Significant compared to FA within same strain exposure groups.

\*\* Significant compared to UFPM within same strain exposure groups.

# Significant compared to O<sub>3</sub> within same strain exposure groups.

Table IV. White Blood Cell, Platelet Aggregate and Platelet-White Cell Aggregates Flow Cytometry Percent-Positive and Mean Fluorescence Intensity (means  $\pm$  SEM).

Parameter	NW				SH			
	FA	UFPM	O <sub>3</sub>	UFPM+O <sub>3</sub>	FA	UFPM	O <sub>3</sub>	UFPM+O <sub>3</sub>
CD61 %+	64.41 $\pm$ 5.065	59.47 $\pm$ 6.301	59.52 $\pm$ 10.14	45.65 $\pm$ 4.21 7	65.93 $\pm$ 6.491	36.14 $\pm$ 9.85	70.16 $\pm$ 7.543	24.72 $\pm$ 6.73 8
CD11b %+	16.75 $\pm$ 1.869	9.744 $\pm$ 1.965	15.43 $\pm$ 6.377	9.262 $\pm$ 1.19 6	20.54 $\pm$ 3.758	8.801 $\pm$ 3.61 6	23.97 $\pm$ 9.529	5.559 $\pm$ 1.58 7
CD18 %+	19.19 $\pm$ 3.09	11.45 $\pm$ 1.712	14.38 $\pm$ 2.565	13.79 $\pm$ 2.05 9	24.28 $\pm$ 5.052	9.656 $\pm$ 3.75 9	27.22 $\pm$ 9.557	5.521 $\pm$ 1.46
CD61/11b %+	9.916 $\pm$ 2.203	4.154 $\pm$ 6.671	5.894 $\pm$ 1.566	5.034 $\pm$ 8.892 8	12.2 $\pm$ 2.442	7.069 $\pm$ 3.37 4	20.81 $\pm$ 9.188	4.873 $\pm$ 1.43 9
CD61/18 %+	10.72 $\pm$ 2.329	4.557 $\pm$ 5.869	7.224 $\pm$ 2.113	6.166 $\pm$ 9.979 3	14.55 $\pm$ 3.315	7.758 $\pm$ 3.41 4	22.54 $\pm$ 9.124	4.626 $\pm$ 1.41 9
CD61 MFI	79776 $\pm$ 9605	97168 $\pm$ 4604	107067 $\pm$ 213 30	81621 $\pm$ 472 6	93414 $\pm$ 1082 4	51934 $\pm$ 128 16	212420 $\pm$ 1323 46	53966 $\pm$ 945 2
CD11b MFI	140341 $\pm$ 302 31	111984 $\pm$ 256 19	111984 $\pm$ 256 19	91222 $\pm$ 180 85	110938 $\pm$ 155 20	72511 $\pm$ 211 26	86738 $\pm$ 10606	40162 $\pm$ 160 95
CD18 MFI	9575 $\pm$ 1296	8133 $\pm$ 2420	6935 $\pm$ 619.2	5492 $\pm$ 709. 1	8120 $\pm$ 599.7	5643 $\pm$ 1179	6243 $\pm$ 689.6	5643 $\pm$ 1179

Normal Wistar rat (NW); Spontaneously Hypertensive rat (SH); filtered air (FA); ultrafine particulate matter (UFPM); ozone (O<sub>3</sub>); ultrafine particulate matter combined with ozone (UFPM+O<sub>3</sub>); percent-positive (%+); mean fluorescence intensity (MFI); the Kruskal-Wallis test was used to calculate the difference between exposure groups by strain and significant *p*-values (*p* < 0.05) from Dunn-Bonferroni post-hoc test are shown in table. Values are shown as the means  $\pm$  SEM by exposure group and strain.

\* Significant compared to FA within same strain exposure groups.

\*\* Significant compared to UFPM within same strain exposure groups.

# Significant compared to O<sub>3</sub> within same strain exposure groups.

### **E. Heart Rate Variability Results:**

All data below are separated by strain (Normal Wistar vs Spontaneously Hypertensive Rats). There is evidence in the literature of an association between the propensity for lethal arrhythmias and signs of increased sympathetic or reduced vagal activity. HRV studies are quantitative markers and assessments of autonomic neural activity. We have defined HRV as the oscillation in the interval between consecutive heart beats as well as the oscillations between consecutive instantaneous heart rates. HRV was analyzed using time- and frequency-domain parameters.

*Time-domain methods.* The detrended RR interval time series data was assessed for the standard deviation of RR interval (SDRR), an estimation of overall HRV, the integral of the RR interval histogram divided by the height of the histogram (HRVti), an estimation of overall HRV, and the square root of mean squared differences of successive RR intervals (RMSSD) high frequency, an estimation of the short-term components of HRV. Considerations of SDRR, RMSSD, and HRVti during exposure and recovery demonstrated that there were significant differences in a number of exposure conditions. In comparison to baseline values, NW rats showed significant differences for all 3 parameters in response to UFPM+O<sub>3</sub> ( $p < 0.05$ ). However, SH rats showed significant differences from baseline for all 3 parameters in response to O<sub>3</sub> as well as UFPM+O<sub>3</sub> ( $p < 0.05$ ).

*Frequency Domain.* The magnitude of HRV in each frequency band is expressed as power, thus we examined the total power of the RR interval data derived from PSD curve. Total power and power in each frequency band has been shown to vary considerably among healthy subjects – thus direct comparisons are misleading. Please note that the power (total and frequency components) are expressed in normalized units, thus it is NOT an absolute measure. Low- and high-frequency band peak frequencies are the highest Hz value identified during sampling period, and reflects the interplay of autonomic interaction. It is not a static parameter nor is it consistent over time.

Figure 7. Time-varying HRV analysis for time-domain parameters in normal and spontaneously hypertensive rats during exposure protocol. (A) Standard deviation of the RR interval (SDRR) for NW and (B) SH rats. (C) Square root of the mean squared differences of successive RR intervals (RMSSD) for NW and (D) SH rats. (E) HRV triangular index (HRVti) for NW and (F) SH rats.

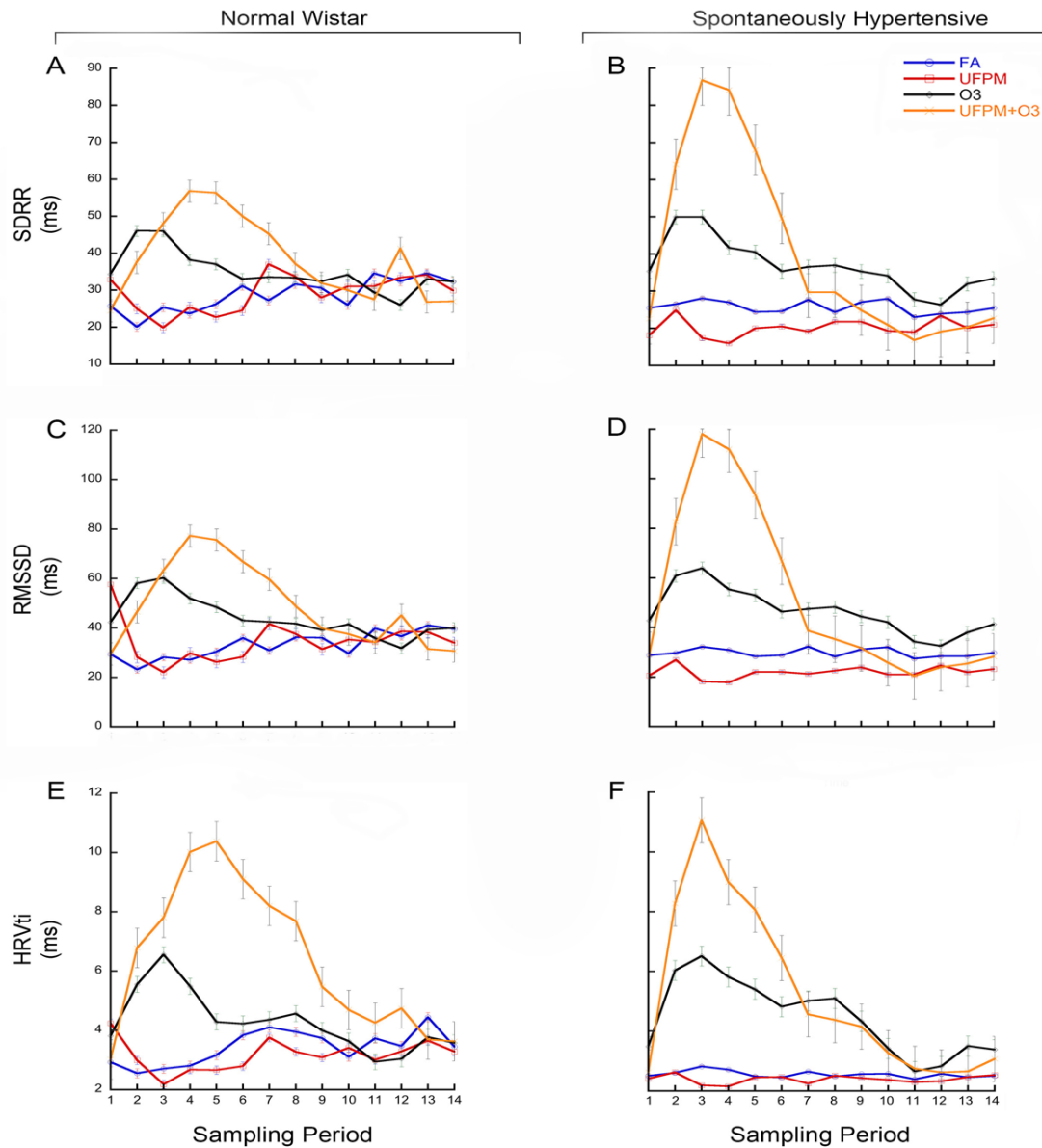


Figure 8: Time-varying HRV analysis for frequency-domain parameters in normal and spontaneously hypertensive rats during exposure protocol. (A) LF peak for NW and (B) SH rats. (C) HF peak for NW and (D) SH rats.

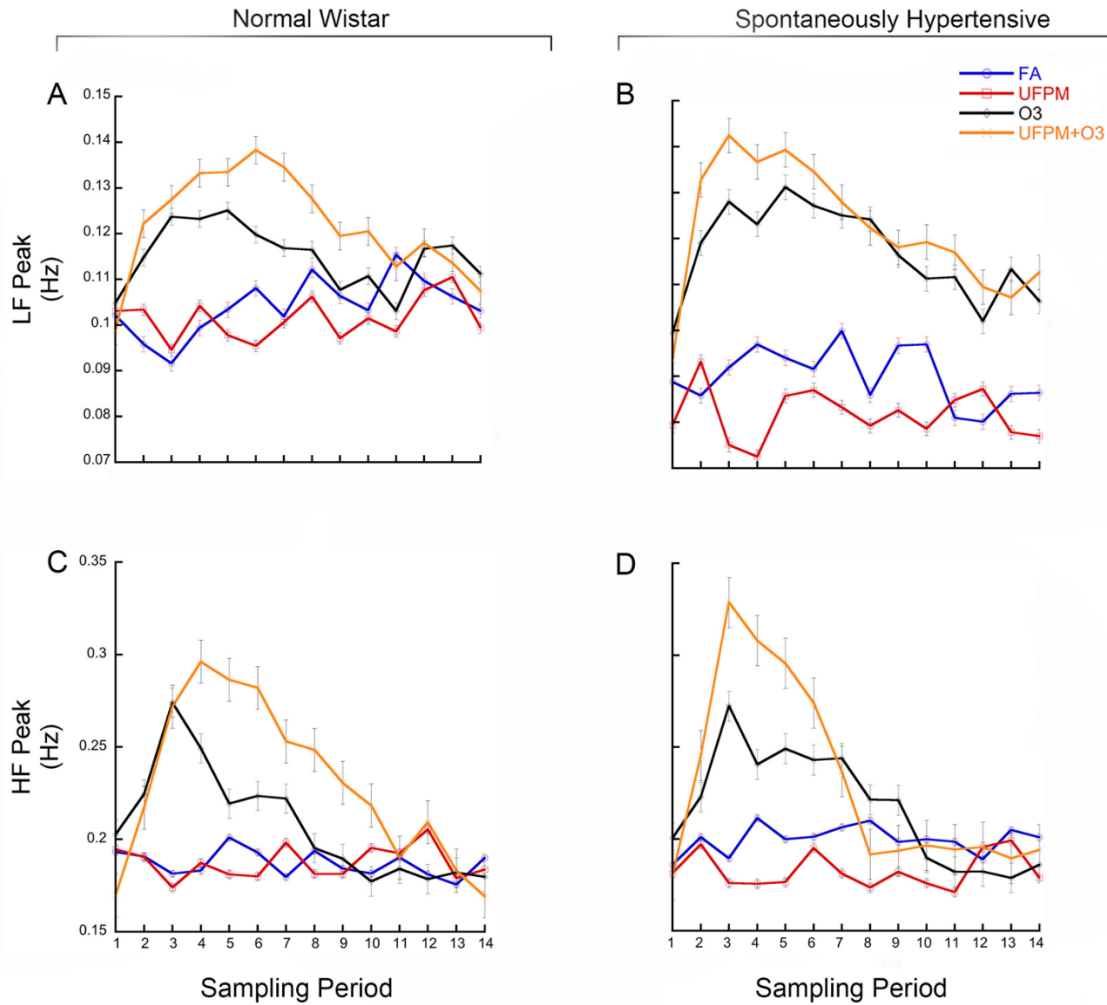


Figure 9: Time-varying HRV analysis for frequency-domain parameters in NW and SH rats during exposure protocol. (A) Normalized LF values for NW and (B) SH rats. (C) Normalized HF values for NW and (D) SH rats. (E) LF/HF ratio for NW and (F) SH rats.

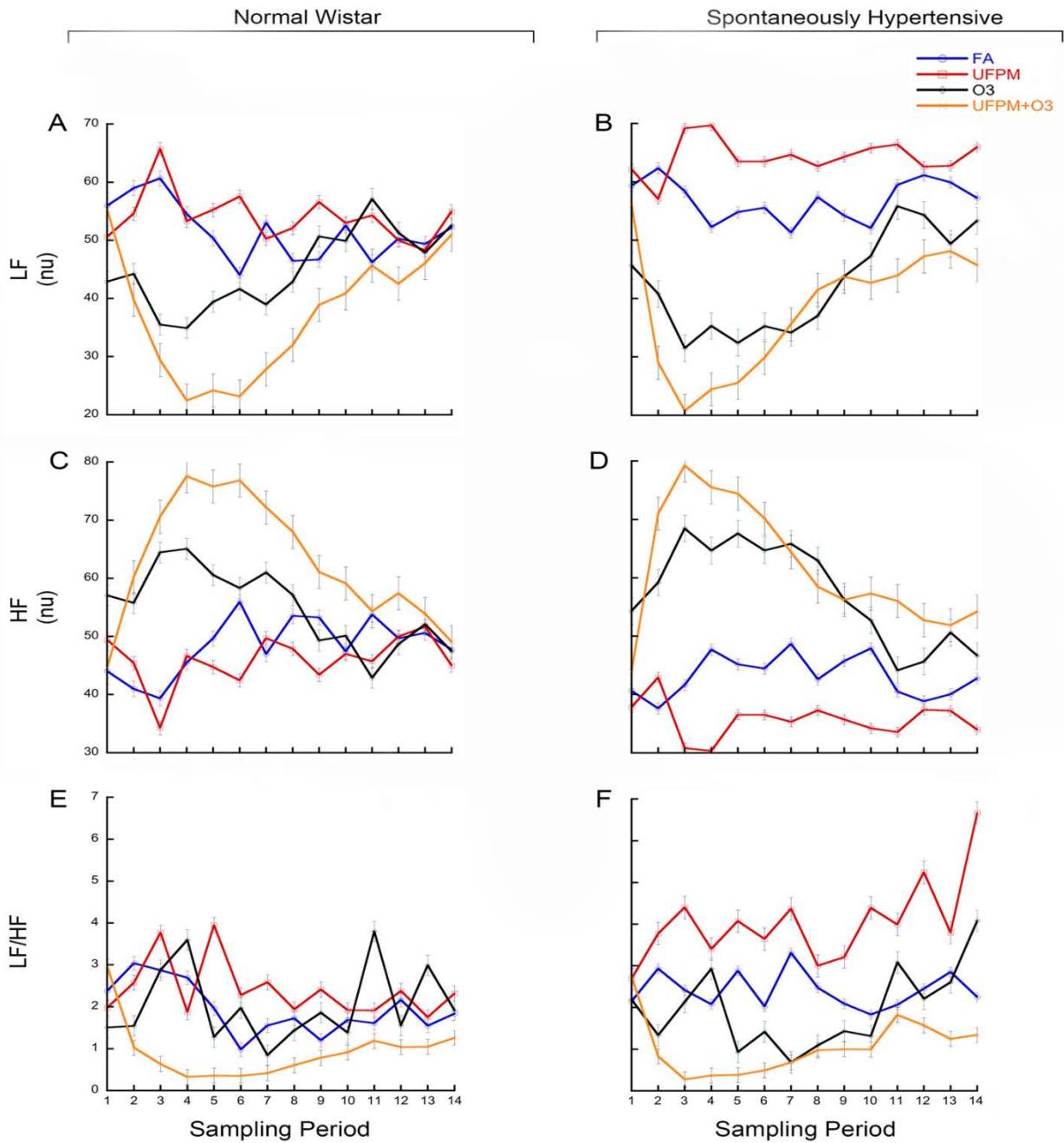


Table V. Time-varying values for the standard deviation of the RR interval (SDRR) in normal and spontaneously hypertensive rats during exposure (mean  $\pm$  SEM).

Timepoint	NW				SH			
	FA	UFPM	O <sub>3</sub>	UFPM+O <sub>3</sub>	FA	UFPM	O <sub>3</sub>	UFPM+O <sub>3</sub>
Baseline	25.8 $\pm$ 2.5	32.9 $\pm$ 11.5	34.3 $\pm$ 1.3	24.5 $\pm$ 4.0	25.5 $\pm$ 3.4	18.1 $\pm$ 2.2	35.4 $\pm$ 1.2	22.6 $\pm$ 2.8
E1	20.1 $\pm$ 3.8	25.0 $\pm$ 6.2	46.0 $\pm$ 3.3*	37.6 $\pm$ 3.3*	26.5 $\pm$ 2.9	24.9 $\pm$ 3.1	50.0 $\pm$ 3.8*	64.2 $\pm$ 5.7**
E2	25.4 $\pm$ 3.4	19.9 $\pm$ 2.5	46.0 $\pm$ 2.4	48.0 $\pm$ 4.0*	28.1 $\pm$ 3.0	17.4 $\pm$ 2.0	50.0 $\pm$ 3.1**	86.8 $\pm$ 7.8**
E3	23.7 $\pm$ 2.2	25.5 $\pm$ 7.3	38.2 $\pm$ 2.6	56.8 $\pm$ 2.1*	27.0 $\pm$ 1.5	16.0 $\pm$ 1.8	41.7 $\pm$ 2.9**	84.2 $\pm$ 10.2**
E4	26.2 $\pm$ 3.6	22.7 $\pm$ 3.7	37.0 $\pm$ 8.3	56.4 $\pm$ 7.9*	24.4 $\pm$ 1.9	20.0 $\pm$ 2.9	40.5 $\pm$ 5.9**	68.0 $\pm$ 10.9*
E5	31.2 $\pm$ 5.6	24.5 $\pm$ 4.6	33.1 $\pm$ 8.6	50.1 $\pm$ 4.4	24.6 $\pm$ 2.0	20.5 $\pm$ 3.7	35.4 $\pm$ 5.7**	49.6 $\pm$ 7.7*
E6	27.3 $\pm$ 6.4	37.1 $\pm$ 7.4	33.5 $\pm$ 6.1	45.3 $\pm$ 3.6	27.7 $\pm$ 2.5	19.1 $\pm$ 3.6	36.5 $\pm$ 4.5**	29.7 $\pm$ 6.5**
R1	31.2 $\pm$ 3.1	33.8 $\pm$ 7.6	33.4 $\pm$ 7.7	37.2 $\pm$ 4.7	24.3 $\pm$ 1.4	21.7 $\pm$ 4.2	37.0 $\pm$ 6.6*	29.7 $\pm$ 9.4
R2	30.6 $\pm$ 6.5	28.0 $\pm$ 6.9	32.5 $\pm$ 6.5	32.0 $\pm$ 3.7	27.0 $\pm$ 1.4	21.8 $\pm$ 5.2	35.3 $\pm$ 6.5	24.9 $\pm$ 6.1
R3	26.0 $\pm$ 2.6	31.0 $\pm$ 7.8	34.2 $\pm$ 3.8	30.0 $\pm$ 4.4	27.9 $\pm$ 2.2	19.3 $\pm$ 5.3	34.1 $\pm$ 2.7	20.9 $\pm$ 3.2
R4	34.6 $\pm$ 3.7	31.1 $\pm$ 6.2	29.4 $\pm$ 5.3	27.5 $\pm$ 4.4	23.0 $\pm$ 1.4**	19.0 $\pm$ 3.0**	27.7 $\pm$ 4.1	16.8 $\pm$ 2.7**
R5	32.4 $\pm$ 4.3	33.4 $\pm$ 7.5	26.0 $\pm$ 4.0	41.3 $\pm$ 11.4	23.9 $\pm$ 2.3	23.4 $\pm$ 3.6	26.3 $\pm$ 2.8	19.1 $\pm$ 4.7**
R6	34.6 $\pm$ 6.8	34.1 $\pm$ 8.4	33.0 $\pm$ 11.2	26.8 $\pm$ 6.5	24.3 $\pm$ 1.4	3.0 $\pm$ 5.2	31.9 $\pm$ 7.1	20.3 $\pm$ 3.8
R7	32.3 $\pm$ 5.5	29.9 $\pm$ 8.9	32.3 $\pm$ 5.7	27.0 $\pm$ 7.0	25.4 $\pm$ 2.6	21.0 $\pm$ 4.4	33.4 $\pm$ 5.4	22.8 $\pm$ 7.6

Table V. Normal Wistar-Kyoto rat (NW); Spontaneously Hypertensive rat (SH); filtered air (FA); ultrafine particulate matter (UFPM); ozone (O<sub>3</sub>); ultrafine particulate matter combined with ozone (UFPM+O<sub>3</sub>); hour of exposure (Ex [ $\chi$ =1-6]); hour of recovery (Rx [ $\chi$ =1-7]); a mixed model three-way ANOVA was used to calculate the differences between exposure groups by strain. The Bonferroni post-hoc test was applied to results for significant  $p$ -values ( $p < 0.05$ ), and indicated above. Values are shown as the means  $\pm$  SEM by exposure group and strain.

\* Significant compared to FA within same strain exposure groups.

\*\* Significant difference between NW and SH within same strain exposure groups.

Table VI. Time-varying values for the square root of the mean squared differences of successive RR intervals (RMSSD) in normal and spontaneously hypertensive rats during exposure (mean  $\pm$  SEM).

Timepoint	NW				SH			
	FA	UFPM	O <sub>3</sub>	UFPM+O <sub>3</sub>	FA	UFPM	O <sub>3</sub>	UFPM+O <sub>3</sub>
Baseline	29.3 $\pm$ 3.1	39.6 $\pm$ 20.2	42.3 $\pm$ 1.3	29.5 $\pm$ 5.6	28.2 $\pm$ 4.0	20.6 $\pm$ 2.8	42.8 $\pm$ 0.9	28.8 $\pm$ 3.8
E1	23.2 $\pm$ 4.7	28.2 $\pm$ 7.4	58.1 $\pm$ 6.8*	46.5 $\pm$ 4.6*	29.7 $\pm$ 3.3	26.9 $\pm$ 4.2	60.9 $\pm$ 5.1*	82.8 $\pm$ 9.2**
E2	28.2 $\pm$ 3.6	22.0 $\pm$ 2.7	60.2 $\pm$ 4.1	63.6 $\pm$ 7.0*	32.2 $\pm$ 3.5	18.1 $\pm$ 2.5	64.0 $\pm$ 3.7**	118.1 $\pm$ 12.9**
E3	27.1 $\pm$ 2.1	29.8 $\pm$ 8.8	51.9 $\pm$ 4.3	77.3 $\pm$ 3.6*	30.9 $\pm$ 1.8	17.8 $\pm$ 2.2	55.3 $\pm$ 3.5**	112.0 $\pm$ 15.6**
E4	30.4 $\pm$ 3.7	26.2 $\pm$ 4.4	48.4 $\pm$ 11.4	75.6 $\pm$ 10.7*	28.3 $\pm$ 2.1	22.0 $\pm$ 3.2	53.0 $\pm$ 7.8**	93.5 $\pm$ 16.3*
E5	36.0 $\pm$ 6.4	28.3 $\pm$ 6.2	43.0 $\pm$ 12.8	66.8 $\pm$ 6.0	28.8 $\pm$ 2.3	22.1 $\pm$ 4.0	46.3 $\pm$ 8.4**	66.7 $\pm$ 11.2*
E6	30.9 $\pm$ 6.8	41.6 $\pm$ 9.1	42.4 $\pm$ 8.8	59.7 $\pm$ 5.1	32.3 $\pm$ 3.0	21.3 $\pm$ 4.4	47.5 $\pm$ 6.8**	38.7 $\pm$ 8.7
R1	36.2 $\pm$ 3.6	37.6 $\pm$ 8.3	41.7 $\pm$ 10.1	48.7 $\pm$ 6.8	28.2 $\pm$ 1.9	22.5 $\pm$ 4.5	48.2 $\pm$ 9.4**	35.3 $\pm$ 10.0
R2	36.0 $\pm$ 7.9	31.4 $\pm$ 8.2	39.1 $\pm$ 7.8	39.8 $\pm$ 5.3	31.1 $\pm$ 1.3	23.9 $\pm$ 5.8	44.4 $\pm$ 9.1	31.7 $\pm$ 8.1
R3	29.6 $\pm$ 3.1	35.3 $\pm$ 9.2	41.5 $\pm$ 5.2	37.5 $\pm$ 6.2	32.1 $\pm$ 2.2	21.1 $\pm$ 6.0	42.1 $\pm$ 4.0	25.8 $\pm$ 4.1
R4	39.8 $\pm$ 4.1	34.2 $\pm$ 6.9	35.9 $\pm$ 6.5	34.1 $\pm$ 5.7	27.4 $\pm$ 1.7	21.0 $\pm$ 3.8	34.3 $\pm$ 5.1	20.5 $\pm$ 3.4**
R5	36.6 $\pm$ 4.8	38.6 $\pm$ 9.2	31.8 $\pm$ 4.4	45.1 $\pm$ 12.3	28.3 $\pm$ 3.0	24.7 $\pm$ 3.6	32.5 $\pm$ 3.2	23.9 $\pm$ 6.5**
R6	41.1 $\pm$ 7.8	38.3 $\pm$ 9.7	39.3 $\pm$ 13.8	31.5 $\pm$ 8.7	28.4 $\pm$ 1.8	21.9 $\pm$ 6.0	38.0 $\pm$ 8.8	25.4 $\pm$ 4.9
R7	39.6 $\pm$ 7.6	34.0 $\pm$ 10.7	40.0 $\pm$ 7.3	30.7 $\pm$ 8.9	29.8 $\pm$ 3.2	23.2 $\pm$ 5.0	41.3 $\pm$ 6.7	28.2 $\pm$ 10.3

Table VI. Normal Wistar-Kyoto rat (NW); Spontaneously Hypertensive rat (SH); filtered air (FA); ultrafine particulate matter (UFPM); ozone (O<sub>3</sub>); ultrafine particulate matter combined with ozone (UFPM+O<sub>3</sub>); hour of exposure (Ex [ $\chi$ =1-6]); hour of recovery (Rx[ $\chi$ =1-7]); a mixed model three-way ANOVA was used to calculate the differences between exposure groups by strain. The Bonferroni post-hoc test was applied to results for significant  $p$ -values ( $p < 0.05$ ), and indicated above. Values are shown as the means  $\pm$  SEM by exposure group and strain.

\* Significant compared to FA within same strain exposure groups.

\*\* Significant difference between NW and SH within same strain exposure groups.

Table VII. Time-varying values for the HRV triangular index (HRVti) in normal and spontaneously hypertensive rats during exposure (mean  $\pm$  SEM).

Timepoint	NW				SH			
	FA	UFPM	O <sub>3</sub>	UFPM+O <sub>3</sub>	FA	UFPM	O <sub>3</sub>	UFPM+O <sub>3</sub>
Baseline	2.9 $\pm$ 0.2	4.2 $\pm$ 1.1	3.8 $\pm$ 0.8	3.0 $\pm$ 0.3	2.5 $\pm$ 0.2	2.4 $\pm$ 0.1	3.5 $\pm$ 0.6	2.6 $\pm$ 0.3
E1	2.6 $\pm$ 0.3	3.0 $\pm$ 0.4	5.5 $\pm$ 1.3*	6.8 $\pm$ 0.5*	2.6 $\pm$ 0.2	2.6 $\pm$ 0.1	6.0 $\pm$ 0.9*	8.3 $\pm$ 1.1*
E2	2.7 $\pm$ 0.2	2.2 $\pm$ 0.1	6.6 $\pm$ 1.8	7.8 $\pm$ 0.7*	2.8 $\pm$ 0.2	2.2 $\pm$ 0.1	6.5 $\pm$ 1.2*	11.1 $\pm$ 1.2**,
E3	2.8 $\pm$ 0.3	2.7 $\pm$ 0.4	5.5 $\pm$ 1.0	10.0 $\pm$ 0.6*	2.7 $\pm$ 0.1	2.2 $\pm$ 0.1	5.8 $\pm$ 0.9**,	9.0 $\pm$ 1.6*
E4	3.2 $\pm$ 0.4	2.7 $\pm$ 0.4	4.3 $\pm$ 0.8	10.4 $\pm$ 1.0*	2.5 $\pm$ 0.1	2.5 $\pm$ 0.2	5.4 $\pm$ 0.9**,	8.1 $\pm$ 1.3*
E5	3.8 $\pm$ 0.6	2.8 $\pm$ 0.3	4.2 $\pm$ 1.0	9.1 $\pm$ 0.8*	2.4 $\pm$ 0.1	2.5 $\pm$ 0.3	4.8 $\pm$ 0.7**,	6.5 $\pm$ 1.1**,
E6	4.1 $\pm$ 1.4	3.8 $\pm$ 0.6	4.4 $\pm$ 0.8	8.2 $\pm$ 1.0	2.6 $\pm$ 0.2	2.2 $\pm$ 0.2	5.0 $\pm$ 0.7**,	4.6 $\pm$ 0.9**
R1	3.9 $\pm$ 0.7	3.3 $\pm$ 0.7	4.6 $\pm$ 1.2	7.7 $\pm$ 1.3	2.5 $\pm$ 0.1	2.5 $\pm$ 0.3	5.1 $\pm$ 1.0*	4.4 $\pm$ 0.8**
R2	3.7 $\pm$ 0.8	3.1 $\pm$ 0.5	4.0 $\pm$ 0.7	5.5 $\pm$ 0.9	2.6 $\pm$ 0.1	2.4 $\pm$ 0.3	4.3 $\pm$ 0.8	4.2 $\pm$ 0.9
R3	3.1 $\pm$ 0.3	3.4 $\pm$ 0.7	3.6 $\pm$ 0.7	4.7 $\pm$ 0.6	2.6 $\pm$ 0.2	2.4 $\pm$ 0.3	3.4 $\pm$ 0.5	3.3 $\pm$ 0.5**
R4	3.7 $\pm$ 0.3	3.0 $\pm$ 0.4	2.9 $\pm$ 0.2	4.3 $\pm$ 1.0	2.4 $\pm$ 0.1	2.3 $\pm$ 0.1	2.7 $\pm$ 0.2	2.7 $\pm$ 0.3**
R5	3.5 $\pm$ 0.5	3.3 $\pm$ 0.5	3.0 $\pm$ 0.4	4.7 $\pm$ 0.7	2.6 $\pm$ 0.1**	2.3 $\pm$ 0.2	2.8 $\pm$ 0.3	2.6 $\pm$ 0.4**
R6	4.4 $\pm$ 0.6	3.7 $\pm$ 0.6	3.8 $\pm$ 0.6	3.7 $\pm$ 0.6	2.5 $\pm$ 0.1	2.5 $\pm$ 0.3	3.5 $\pm$ 0.5	2.7 $\pm$ 0.3
R7	3.4 $\pm$ 0.4	3.3 $\pm$ 0.6	3.6 $\pm$ 0.4	3.6 $\pm$ 0.7	2.5 $\pm$ 0.2	2.5 $\pm$ 0.2	3.4 $\pm$ 0.4	3.1 $\pm$ 0.7

Table VII. Heart rate variability (HRV); normal Wistar-Kyoto rat (NW); Spontaneously Hypertensive rat (SH); filtered air (FA); ultrafine particulate matter (UFPM); ozone (O<sub>3</sub>); ultrafine particulate matter combined with ozone (UFPM+O<sub>3</sub>); hour of exposure (Ex [x=1-6]); hour of recovery (Rx[x=1-7]); a mixed model three-way ANOVA was used to calculate the differences between exposure groups by strain. The Bonferroni post-hoc test was applied to results for significant *p*-values (*p* < 0.05), and indicated above. Values are shown as the means  $\pm$  SEM by exposure group and strain.

\* Significant compared to FA within same strain exposure groups.

\*\* Significant difference between NW and SH within same strain exposure groups.

Table VIII. Time-varying values for normalized low frequency (LF [n.u.]) in normal and spontaneously hypertensive rats during exposure (mean  $\pm$  SEM).

Timepoint	NW				SH			
	FA	UFPM	O <sub>3</sub>	UFPM+O <sub>3</sub>	FA	UFPM	O <sub>3</sub>	UFPM+O <sub>3</sub>
Baseline	55.9 $\pm$ 2.2	50.6 $\pm$ 6.7	42.9 $\pm$ 3.5	55.3 $\pm$ 4.2	59.4 $\pm$ 3.3	62.2 $\pm$ 2.7	45.7 $\pm$ 3.0	56.1 $\pm$ 4.0
E1	59.0 $\pm$ 4.0	54.6 $\pm$ 3.7	44.2 $\pm$ 8.2	39.8 $\pm$ 4.4	62.4 $\pm$ 4.3	57.1 $\pm$ 4.6	40.8 $\pm$ 7.4 <sup>***</sup>	29.0 $\pm$ 6.1 <sup>*</sup>
E2	60.6 $\pm$ 2.0	65.8 $\pm$ 3.9	35.5 $\pm$ 10.6	29.4 $\pm$ 5.1 <sup>*</sup>	58.4 $\pm$ 3.8	69.2 $\pm$ 2.1	31.5 $\pm$ 7.5 <sup>***</sup>	20.7 $\pm$ 2.0 <sup>*</sup>
E3	54.5 $\pm$ 4.6	53.3 $\pm$ 3.6	34.9 $\pm$ 5.6	22.5 $\pm$ 3.1 <sup>*</sup>	52.3 $\pm$ 4.1	69.7 $\pm$ 2.0 <sup>***</sup>	35.3 $\pm$ 6.0 <sup>*</sup>	24.5 $\pm$ 3.7 <sup>*</sup>
E4	50.4 $\pm$ 4.5	55.3 $\pm$ 2.8	39.4 $\pm$ 4.6	24.2 $\pm$ 3.1 <sup>*</sup>	54.8 $\pm$ 2.3	63.5 $\pm$ 1.8	32.4 $\pm$ 5.6 <sup>***</sup>	25.6 $\pm$ 2.4 <sup>*</sup>
E5	44.1 $\pm$ 3.3	57.6 $\pm$ 4.4	41.6 $\pm$ 6.5	23.2 $\pm$ 3.3 <sup>*</sup>	55.6 $\pm$ 2.6 <sup>**</sup>	63.5 $\pm$ 2.7	35.3 $\pm$ 5.8 <sup>***</sup>	29.6 $\pm$ 3.3 <sup>*</sup>
E6	53.0 $\pm$ 5.9	50.3 $\pm$ 1.6	39.0 $\pm$ 6.0	27.8 $\pm$ 2.3 <sup>*</sup>	51.3 $\pm$ 4.6	64.7 $\pm$ 2.2	34.2 $\pm$ 5.4 <sup>***</sup>	35.6 $\pm$ 5.0
R1	46.5 $\pm$ 2.1	52.1 $\pm$ 2.4	42.9 $\pm$ 5.8	32.0 $\pm$ 4.3	57.4 $\pm$ 2.2	62.7 $\pm$ 3.1	37.0 $\pm$ 6.0 <sup>***</sup>	41.5 $\pm$ 5.1 <sup>*</sup>
R2	46.7 $\pm$ 2.7	56.6 $\pm$ 3.2	50.7 $\pm$ 4.0	38.9 $\pm$ 4.4	54.2 $\pm$ 3.9	64.3 $\pm$ 2.5	43.8 $\pm$ 6.3 <sup>***</sup>	43.7 $\pm$ 4.5
R3	52.6 $\pm$ 3.8	53.0 $\pm$ 4.1	49.9 $\pm$ 5.7	40.9 $\pm$ 5.0	52.1 $\pm$ 3.1	65.8 $\pm$ 3.7	47.3 $\pm$ 4.7	42.7 $\pm$ 5.4
R4	46.2 $\pm$ 1.6	54.3 $\pm$ 2.8	57.1 $\pm$ 3.1	45.7 $\pm$ 4.7	59.5 $\pm$ 3.2 <sup>**</sup>	66.4 $\pm$ 4.6 <sup>**</sup>	55.8 $\pm$ 2.2	44.0 $\pm$ 4.3 <sup>*</sup>
R5	50.3 $\pm$ 2.4	50.0 $\pm$ 3.5	51.3 $\pm$ 2.3	42.6 $\pm$ 4.1	61.1 $\pm$ 1.5 <sup>**</sup>	62.6 $\pm$ 2.8 <sup>**</sup>	54.3 $\pm$ 3.1	47.2 $\pm$ 5.3 <sup>*</sup>
R6	49.4 $\pm$ 2.6	48.3 $\pm$ 2.8	47.9 $\pm$ 4.2	46.1 $\pm$ 3.6	59.9 $\pm$ 2.7 <sup>**</sup>	62.8 $\pm$ 4.2 <sup>**</sup>	49.4 $\pm$ 3.5	48.1 $\pm$ 4.2
R7	52.2 $\pm$ 2.9	55.0 $\pm$ 5.6	52.6 $\pm$ 5.3	51.0 $\pm$ 2.1	57.2 $\pm$ 2.2	66.0 $\pm$ 1.5 <sup>**</sup>	53.4 $\pm$ 3.4	45.8 $\pm$ 1.8

Table VIII. Normal Wistar-Kyoto rat (NW); Spontaneously Hypertensive rat (SH); filtered air (FA); ultrafine particulate matter (UFPM); ozone (O<sub>3</sub>); ultrafine particulate matter combined with ozone (UFPM+O<sub>3</sub>); hour of exposure (Ex [x=1-6]); hour of recovery (Rx[x=1-7]); a mixed model three-way ANOVA was used to calculate the differences between exposure groups by strain. The Bonferroni post-hoc test was applied to results for significant  $p$ -values ( $p < 0.05$ ), and indicated above. Values are shown as the means  $\pm$  SEM by exposure group and strain.

\* Significant compared to FA within same strain exposure groups.

\*\* Significant difference between NW and SH within same strain exposure groups.

Table IX. Time-varying values for normalized high frequency (HF [n.u.]) in normal and spontaneously hypertensive rats during exposure (mean  $\pm$  SEM).

Timepoint	NW				SH			
	FA	UFPM	O <sub>3</sub>	UFPM+O <sub>3</sub>	FA	UFPM	O <sub>3</sub>	UFPM+O <sub>3</sub>
Baseline	44.1 $\pm$ 2.2	49.7 $\pm$ 6.7	57.1 $\pm$ 3.5	44.7 $\pm$ 4.2	40.6 $\pm$ 3.3	37.8 $\pm$ 2.7	54.3 $\pm$ 3.0	43.9 $\pm$ 4.0
E1	41.0 $\pm$ 4.0	45.4 $\pm$ 3.7	55.8 $\pm$ 8.2	60.2 $\pm$ 4.4	37.6 $\pm$ 4.3	42.9 $\pm$ 4.6	59.2 $\pm$ 7.4**	71.0 $\pm$ 6.1*
E2	39.4 $\pm$ 2.0	34.2 $\pm$ 3.9	64.5 $\pm$ 10.6	70.6 $\pm$ 5.1*	41.6 $\pm$ 3.8	30.8 $\pm$ 2.1	68.5 $\pm$ 7.5**	79.3 $\pm$ 2.0*
E3	45.5 $\pm$ 4.6	46.7 $\pm$ 3.6	65.1 $\pm$ 5.6	77.5 $\pm$ 3.1*	47.7 $\pm$ 4.1	30.3 $\pm$ 2.0**	64.7 $\pm$ 6.0*	75.5 $\pm$ 3.7*
E4	49.6 $\pm$ 4.5	44.7 $\pm$ 2.8	60.6 $\pm$ 4.6	75.8 $\pm$ 3.1*	45.2 $\pm$ 2.3	36.5 $\pm$ 1.8	67.6 $\pm$ 5.6**	74.4 $\pm$ 2.4*
E5	55.9 $\pm$ 3.3	42.4 $\pm$ 4.4	58.4 $\pm$ 6.6	76.8 $\pm$ 3.3*	44.4 $\pm$ 2.6**	36.5 $\pm$ 2.7	64.7 $\pm$ 5.8**	70.2 $\pm$ 3.3*
E6	47.0 $\pm$ 5.9	49.7 $\pm$ 1.6	61.0 $\pm$ 6.0	72.2 $\pm$ 2.3*	48.7 $\pm$ 4.6	35.3 $\pm$ 2.2	65.8 $\pm$ 5.4**	64.4 $\pm$ 5.0
R1	53.5 $\pm$ 2.1	47.9 $\pm$ 2.4	57.1 $\pm$ 5.8	68.0 $\pm$ 4.3	42.6 $\pm$ 2.2	37.3 $\pm$ 3.1	63.0 $\pm$ 6.0**	58.5 $\pm$ 5.1*
R2	53.3 $\pm$ 2.7	43.4 $\pm$ 3.2	49.3 $\pm$ 4.0	61.1 $\pm$ 4.4	45.8 $\pm$ 3.9	35.7 $\pm$ 2.5	56.2 $\pm$ 6.3**	56.3 $\pm$ 4.5
R3	47.4 $\pm$ 3.8	47.0 $\pm$ 4.1	50.1 $\pm$ 5.7	59.1 $\pm$ 5.0	47.9 $\pm$ 3.1	34.2 $\pm$ 3.7	52.7 $\pm$ 4.7	57.3 $\pm$ 5.4
R4	53.8 $\pm$ 1.6	45.7 $\pm$ 2.8	42.9 $\pm$ 3.1	54.3 $\pm$ 4.7	40.5 $\pm$ 3.2**	33.6 $\pm$ 4.6**	44.2 $\pm$ 2.2	56.0 $\pm$ 4.3*
R5	49.7 $\pm$ 2.4	50.0 $\pm$ 3.5	48.7 $\pm$ 2.3	57.4 $\pm$ 4.1	38.9 $\pm$ 1.5**	37.4 $\pm$ 2.8**	45.7 $\pm$ 3.1	52.8 $\pm$ 5.3*
R6	50.6 $\pm$ 2.6	51.7 $\pm$ 2.8	52.1 $\pm$ 4.2	53.9 $\pm$ 3.6	40.1 $\pm$ 2.7**	37.2 $\pm$ 4.2**	50.6 $\pm$ 3.5	51.9 $\pm$ 4.2
R7	47.8 $\pm$ 2.9	45.0 $\pm$ 5.6	47.4 $\pm$ 5.3	49.0 $\pm$ 2.1	42.8 $\pm$ 2.2	34.0 $\pm$ 1.5**	46.6 $\pm$ 3.4	54.2 $\pm$ 1.8

Table IX. Normal Wistar-Kyoto rat (NW); Spontaneously Hypertensive rat (SH); filtered air (FA); ultrafine particulate matter (UFPM); ozone (O<sub>3</sub>); ultrafine particulate matter combined with ozone (UFPM+O<sub>3</sub>); hour of exposure (Ex [x=1-6]); hour of recovery (Rx[x=1-7]); a mixed model three-way ANOVA was used to calculate the differences between exposure groups by strain. The Bonferroni post-hoc test was applied to results for significant *p*-values (*p* < 0.05), and indicated above. Values are shown as the means  $\pm$  SEM by exposure group and strain.

\* Significant compared to FA within same strain exposure groups.

\*\* Significant difference between NW and SH within same strain exposure groups.

Table X. Time-varying values for the low frequency, high frequency ratio (LF:HF) in normal and spontaneously hypertensive rats during exposure (mean  $\pm$  SEM).

Timepoint	NW				SH			
	FA	UFPM	O <sub>3</sub>	UFPM+O <sub>3</sub>	FA	UFPM	O <sub>3</sub>	UFPM+O <sub>3</sub>
Baseline	2.4 $\pm$ 0.3	2.0 $\pm$ 0.2	1.5 $\pm$ 0.4	3.0 $\pm$ 1.3	2.1 $\pm$ 0.2	2.7 $\pm$ 0.6	2.2 $\pm$ 0.6	2.7 $\pm$ 0.8
E1	3.0 $\pm$ 0.7	2.6 $\pm$ 0.5	1.5 $\pm$ 0.5	1.0 $\pm$ 0.2	2.9 $\pm$ 0.4	3.8 $\pm$ 1.2	1.3 $\pm$ 0.4	0.8 $\pm$ 0.4
E2	2.9 $\pm$ 0.4	3.8 $\pm$ 1.3	2.9 $\pm$ 2.5	0.6 $\pm$ 0.2	2.4 $\pm$ 0.3	4.4 $\pm$ 1.0	2.1 $\pm$ 1.7	0.3 $\pm$ 0.0*
E3	2.7 $\pm$ 1.2	1.9 $\pm$ 0.3	3.6 $\pm$ 3.1	0.3 $\pm$ 0.1	2.1 $\pm$ 0.3	3.4 $\pm$ 0.4	2.9 $\pm$ 2.1	0.4 $\pm$ 0.1
E4	2.0 $\pm$ 0.5	3.9 $\pm$ 2.1	1.3 $\pm$ 0.5	0.4 $\pm$ 0.1	2.9 $\pm$ 0.4	4.1 $\pm$ 0.7	0.9 $\pm$ 0.4*	0.4 $\pm$ 0.1*
E5	1.0 $\pm$ 0.1	2.3 $\pm$ 0.4	2.0 $\pm$ 1.3	0.3 $\pm$ 0.1	2.0 $\pm$ 0.2**	3.6 $\pm$ 0.7**	1.4 $\pm$ 0.9***	0.5 $\pm$ 0.1*
E6	1.6 $\pm$ 0.3	2.6 $\pm$ 0.7	0.8 $\pm$ 0.2	0.4 $\pm$ 0.0	3.3 $\pm$ 0.9**	4.4 $\pm$ 1.0**	0.7 $\pm$ 0.2*	0.7 $\pm$ 0.2*
R1	1.7 $\pm$ 0.5	1.9 $\pm$ 0.3	1.4 $\pm$ 0.7	0.6 $\pm$ 0.1	2.5 $\pm$ 0.3**	3.0 $\pm$ 0.5	1.1 $\pm$ 0.5*	1.0 $\pm$ 0.3*
R2	1.2 $\pm$ 0.2	2.4 $\pm$ 0.5	1.9 $\pm$ 0.8	0.8 $\pm$ 0.2	2.1 $\pm$ 0.8**	3.2 $\pm$ 0.4	1.4 $\pm$ 0.6*	1.0 $\pm$ 0.2*
R3	1.7 $\pm$ 0.3	1.9 $\pm$ 0.6	1.4 $\pm$ 0.5	0.9 $\pm$ 0.2	1.8 $\pm$ 0.3	4.4 $\pm$ 0.8**	1.3 $\pm$ 0.3	1.0 $\pm$ 0.3
R4	1.6 $\pm$ 0.5	1.9 $\pm$ 0.2	3.8 $\pm$ 1.3	1.2 $\pm$ 0.3	2.1 $\pm$ 0.2	4.0 $\pm$ 0.8	3.1 $\pm$ 0.9	1.8 $\pm$ 1.0
R5	2.2 $\pm$ 0.6	2.4 $\pm$ 0.5	1.6 $\pm$ 0.5	1.0 $\pm$ 0.2	2.5 $\pm$ 0.2	5.2 $\pm$ 1.8**	2.2 $\pm$ 0.7	1.6 $\pm$ 0.6
R6	1.5 $\pm$ 0.3	1.7 $\pm$ 0.6	3.0 $\pm$ 2.0	1.0 $\pm$ 0.2	2.9 $\pm$ 0.5**	3.8 $\pm$ 0.9	2.6 $\pm$ 1.3	1.2 $\pm$ 0.3
R7	1.8 $\pm$ 0.4	2.3 $\pm$ 0.6	1.9 $\pm$ 0.8	1.3 $\pm$ 0.1	2.2 $\pm$ 0.3	6.7 $\pm$ 2.6**	4.1 $\pm$ 2.1	1.3 $\pm$ 0.2

Table X. Normal Wistar-Kyoto rat (NW); Spontaneously Hypertensive rat (SH); filtered air (FA); ultrafine particulate matter (UFPM); ozone (O<sub>3</sub>); ultrafine particulate matter combined with ozone (UFPM+O<sub>3</sub>); hour of exposure (Ex [ $\chi$ =1-6]); hour of recovery (Rx [ $\chi$ =1-7]); a mixed model three-way ANOVA was used to calculate the differences between exposure groups by strain. The Bonferroni post-hoc test was applied to results for significant  $p$ -values ( $p < 0.05$ ), and indicated above. Values are shown as the means  $\pm$  SEM by exposure group and strain.

\* Significant compared to FA within same strain exposure groups.

\*\* Significant difference between NW and SH within same strain exposure groups.

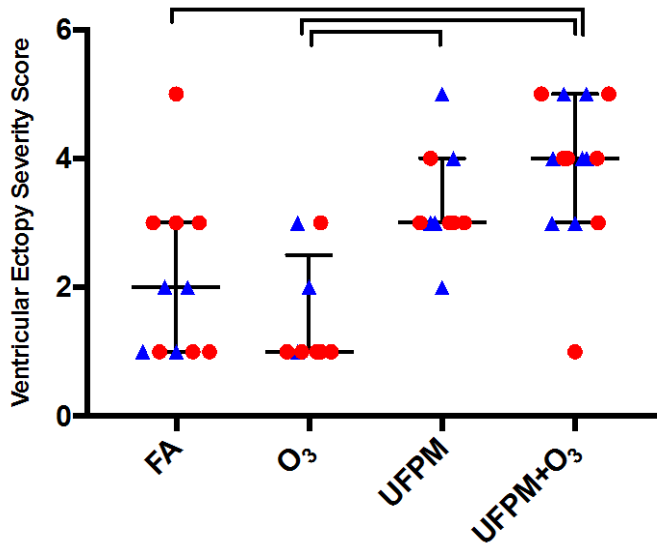
### Electrocardiography Analysis:

It is clear from the figures below, that both rat strains experienced marked increases in arrhythmias associated with UFPM+O<sub>3</sub> exposure. However, exposure to UFPM resulted in significantly increased ventricular ectopic beats. Please note that there were no strain differences seen for any of the arrhythmia parameters.

Please note that NW rats are blue triangles, while SH rats are red circles.

Figure 10: Ventricular Ectopy Severity Score (A) Compared with Total Numbers of VPCs (B).

A. There are statically significant differences between FA and UFPM+O<sub>3</sub>, as well as between O<sub>3</sub> and UFPM+O<sub>3</sub> and between O<sub>3</sub> and UFPM



B. There were significant differences in the total numbers of VPCs between FA and UFPM+O<sub>3</sub> as well as between O<sub>3</sub> and UFPM+O<sub>3</sub>.

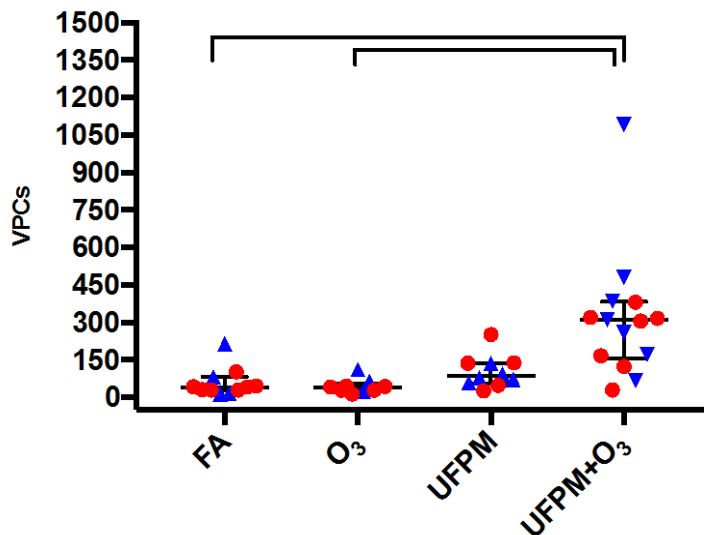


Figure 11: Arrhythmia Severity Score showed significant differences between filtered air and UFPM+O<sub>3</sub> as well as O<sub>3</sub> and UFPM+O<sub>3</sub>.

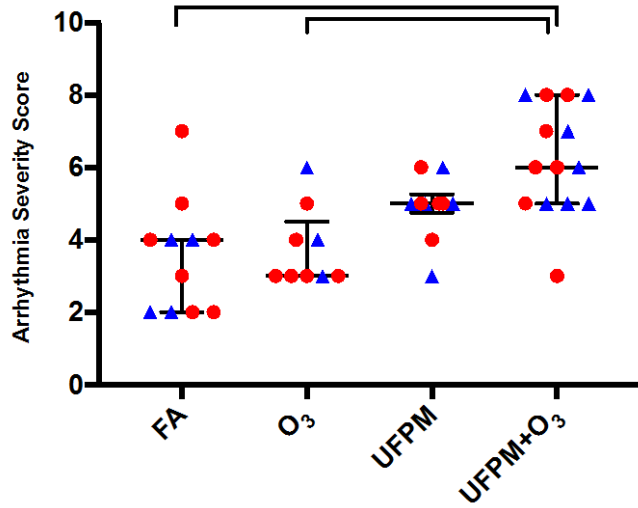


Figure 12: Supraventricular Complexes: There was a statistically significant difference in the severity of supraventricular (SV) complexes between FA and UFPM+O<sub>3</sub>.

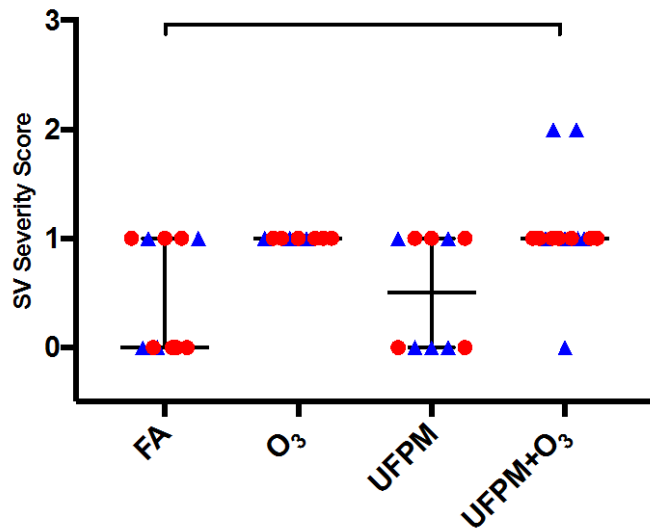


Figure 13: Atrial Premature Complexes: There were significant differences in the total number of APCs between both FA and UFPM+O<sub>3</sub> as well as between O<sub>3</sub> and UFPM+O<sub>3</sub>.

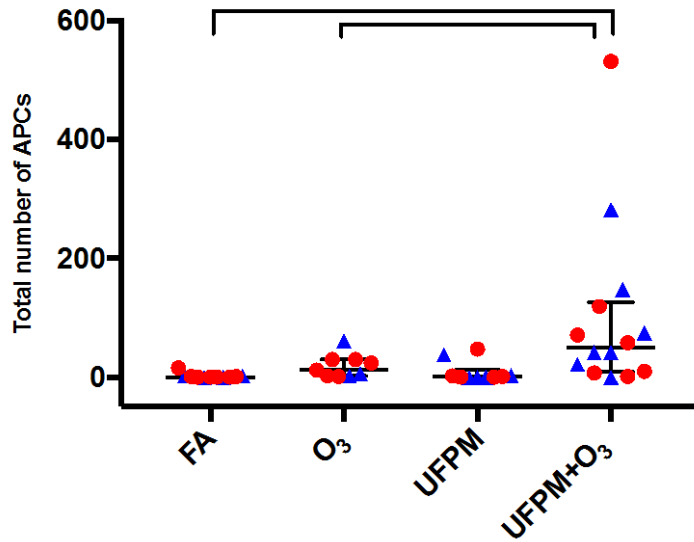


Figure 14: Atrioventricular Block: Similar to the total numbers of APCs, there were significant differences between the total number of AV blocks between FA and UFPM+O<sub>3</sub>.

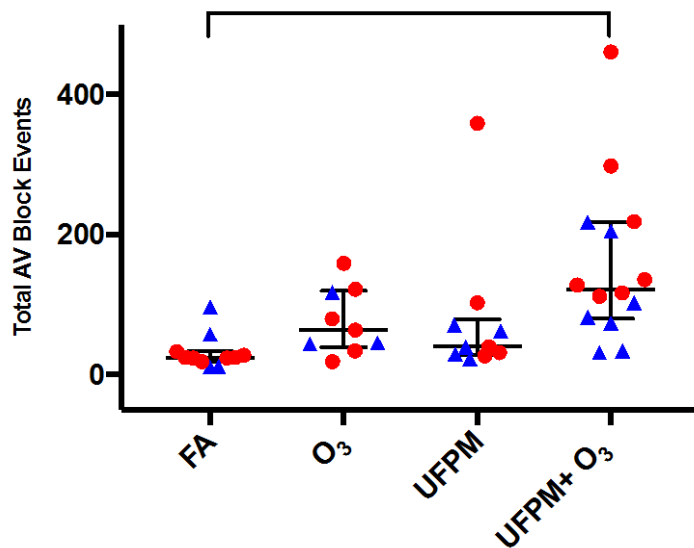


Figure 15: Severity of Atrioventricular Block: There was no statistical difference in the severity of AV block between any of the exposures. AV block was present in both NW and SH rats.

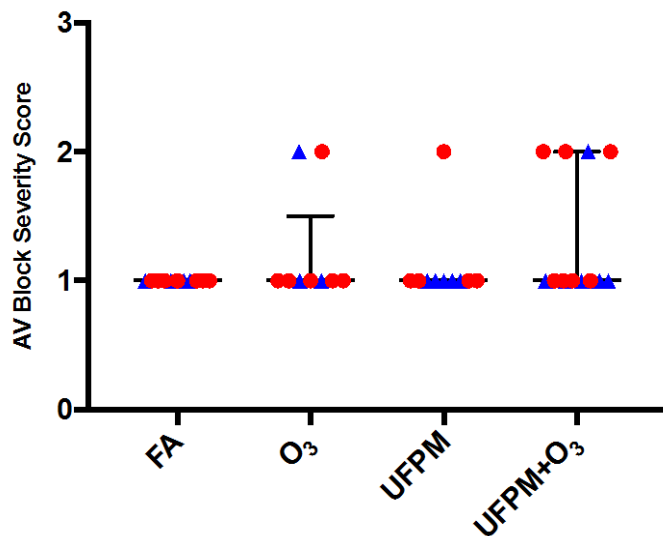


Figure 16.

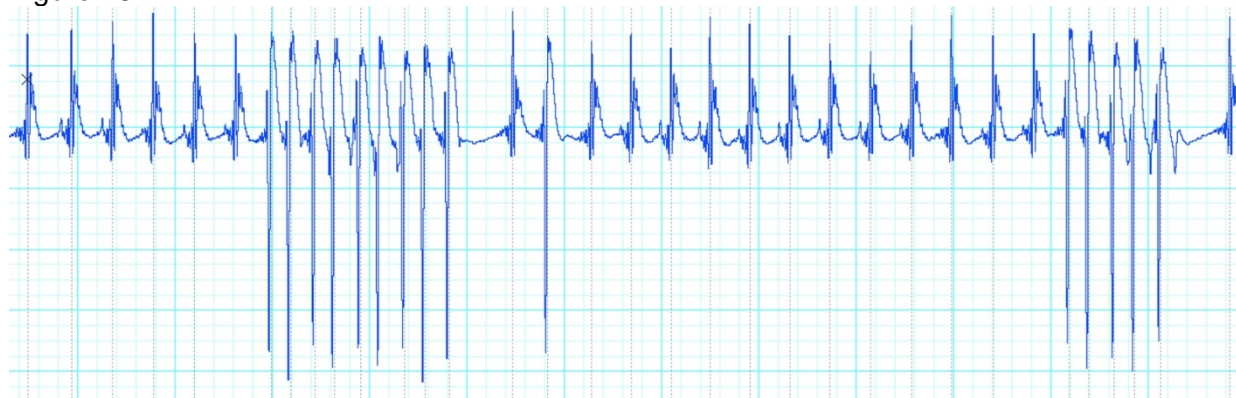


Figure 16. ECG tracing from a UFPM+O<sub>3</sub>-exposed SH rat. The ECG shows multiple severity scale paroxysms of ventricular tachycardia consistent with a grade 5 severity on the ventricular ectopy of this study.

### Histopathology of Heart:

Changes in the myocardium were characterized as acute individual cell necrosis, hyper-eosinophilic and hyper-contracted myocytes, and foci of organized necrosis. Individual necrotic myocytes had shrunken and eosinophilic cytoplasm, evidence of nuclear degeneration and separation from adjacent cells. Hyper-eosinophilic and contracted myocytes maintained connection to adjacent cells, had more intact nuclei but had dense cytoplasm with occasional contraction bands. Foci of organized necrosis consisted of remnants of necrotic myocytes surrounded by a mixed interstitial cell population of mononuclear cells and immature fibroblasts. Lesions were scored based on severity and relative frequency with most changes being evident in the left ventricle and interventricular septum. Myocardial changes were significantly different between SH and NW rats in response to UFPM and UFPM+O<sub>3</sub> (Table VI). Foci of organized necrosis were common in all SH rats with no differences due to exposure group. There was a correlation between the incidence of acute individual necrosis and hyper-contracted myocytes. These lesions were similar and distinction between hyper-contracted and necrotic cells was often unclear. Acute myocyte degenerative or necrotic changes were occasionally present in all rats but the incidence and severity was markedly greater in SH rats exposed to either UFPM alone or UFPM+O<sub>3</sub>. The histology images below of SH rat cardiac lesions show examples of hypercontractility, organized necrosis, and acute cellular necrosis.

Figure 17: Hypercontractility is seen in the image below as highly eosinophilic (pink) cardiac myocytes some of which exhibit sarcomeric banding (→).

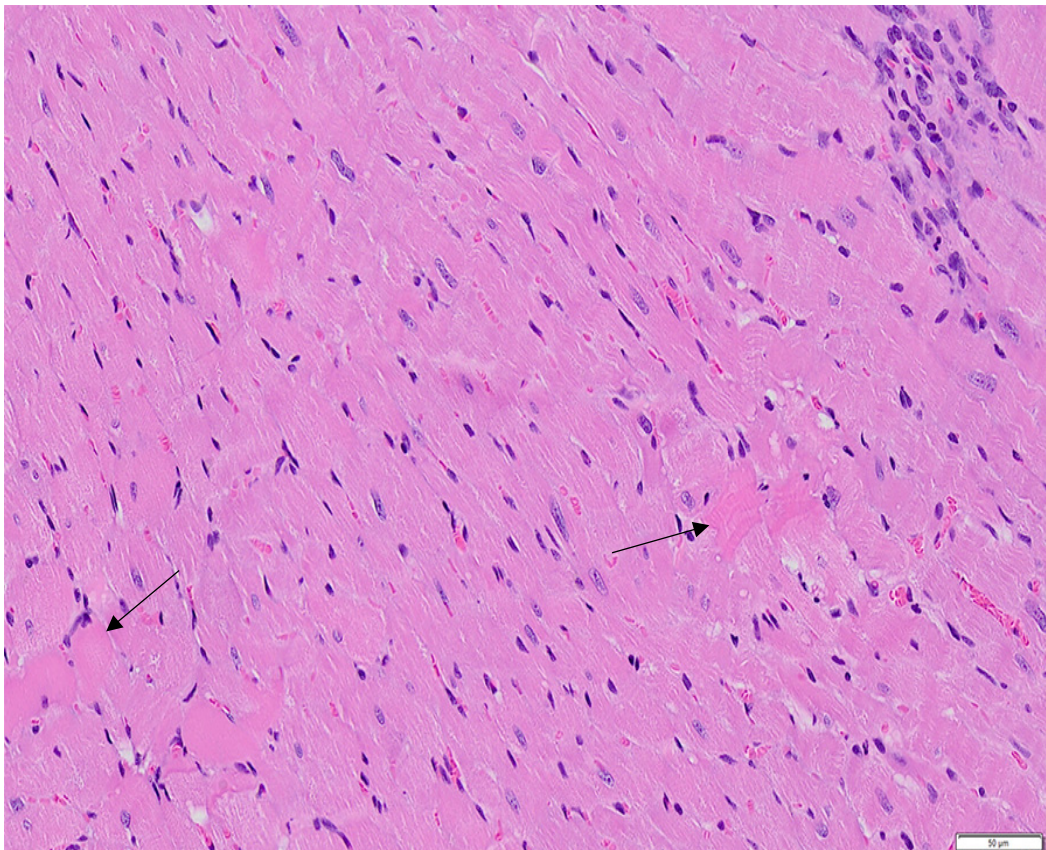


Figure 18: An example of focal organized necrosis (circled area).

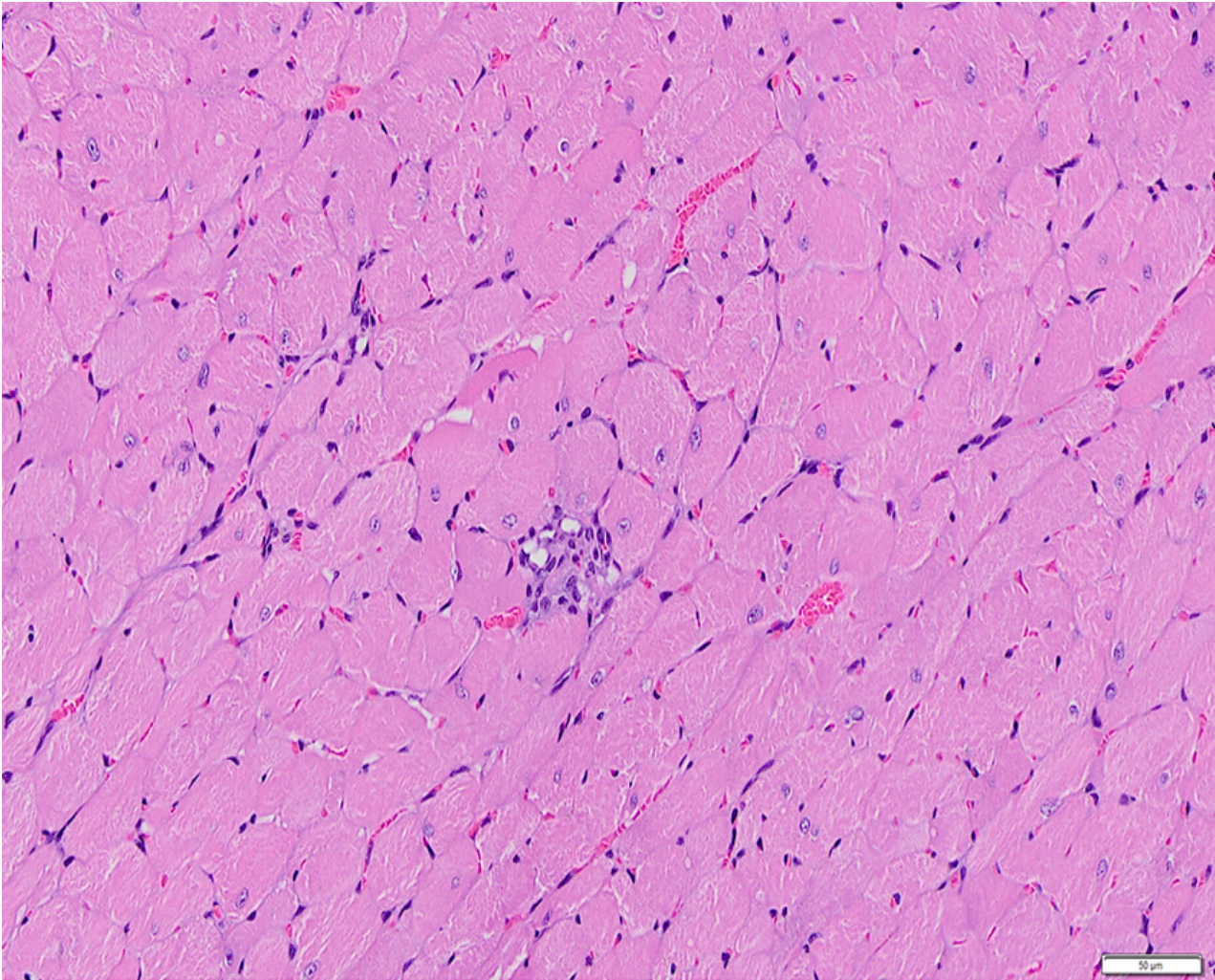


Figure 19: Acute Cellular Necrosis: Individual vacuolated cardiac myocytes (->) can be seen throughout the image.

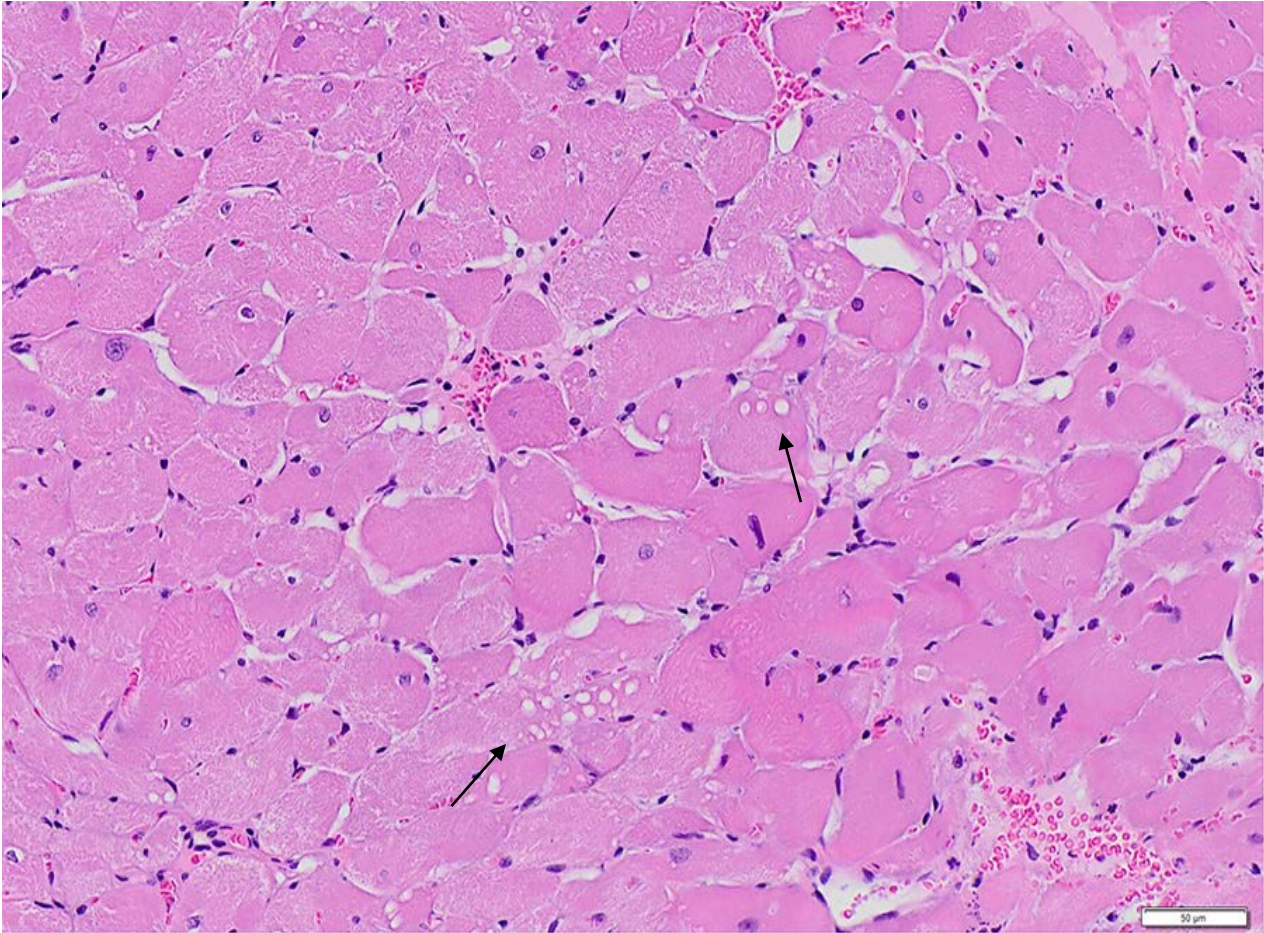


Table XI. Histopathologic measures of the heart in normal and spontaneously hypertensive rats following exposure (mean  $\pm$  SEM).

Parameter	NW				SH			
	FA	UFPM	O <sub>3</sub>	UFPM+O <sub>3</sub>	FA	UFPM	O <sub>3</sub>	UFPM+O <sub>3</sub>
Acute Cellular Necrosis	0.0	0.0	0.1 $\pm$ 0.1	0.3 $\pm$ 0.1	0.0	1.1 $\pm$ 0.3 <sup>##</sup>	0.4 $\pm$ 0.3	2.5 $\pm$ 0.2 <sup>*,**,#,##</sup>
Hypercontractility	0.5 $\pm$ 0.3	0.5 $\pm$ 0.3	0.2 $\pm$ 0.1	0.2 $\pm$ 0.1	0.4 $\pm$ 0.2	1.3 $\pm$ 0.3	0.5 $\pm$ 0.3	1.8 $\pm$ 0.2 <sup>*,##</sup>
Organized Necrosis	0.1 $\pm$ 0.1	0.0	0.0	0.0	0.6 $\pm$ 0.3	1.0 $\pm$ 0.3 <sup>##</sup>	1.0 $\pm$ 0.	0.8 $\pm$ 0.3 <sup>##</sup>

Table XI. Standard, paraffin-embedded, histopathologic sections of lung tissue were evaluated by a board-certified veterinary pathologist for lesions in the large airways, terminal bronchiolar/alveolar duct regions, alveolar parenchyma and vasculature and assigned a severity score (0-5). Note: Normal Wistar rat (NW); Spontaneously Hypertensive rat (SH); filtered air (FA); ultrafine particulate matter (UFPM); ozone (O<sub>3</sub>); ultrafine particulate matter combined with ozone (UFPM+O<sub>3</sub>); the Kruskal-Wallis test was used to calculate the difference between exposure groups by strain and significant *p*-values (*p* < 0.05) from Dunn-Bonferroni post-hoc test are shown in table. Values are shown as the means  $\pm$  SEM by exposure group and strain.

\* Significant compared to FA within same strain exposure groups.

\*\* Significant compared to UFPM within same strain exposure groups.

# Significant compared to O<sub>3</sub> within same strain exposure groups.

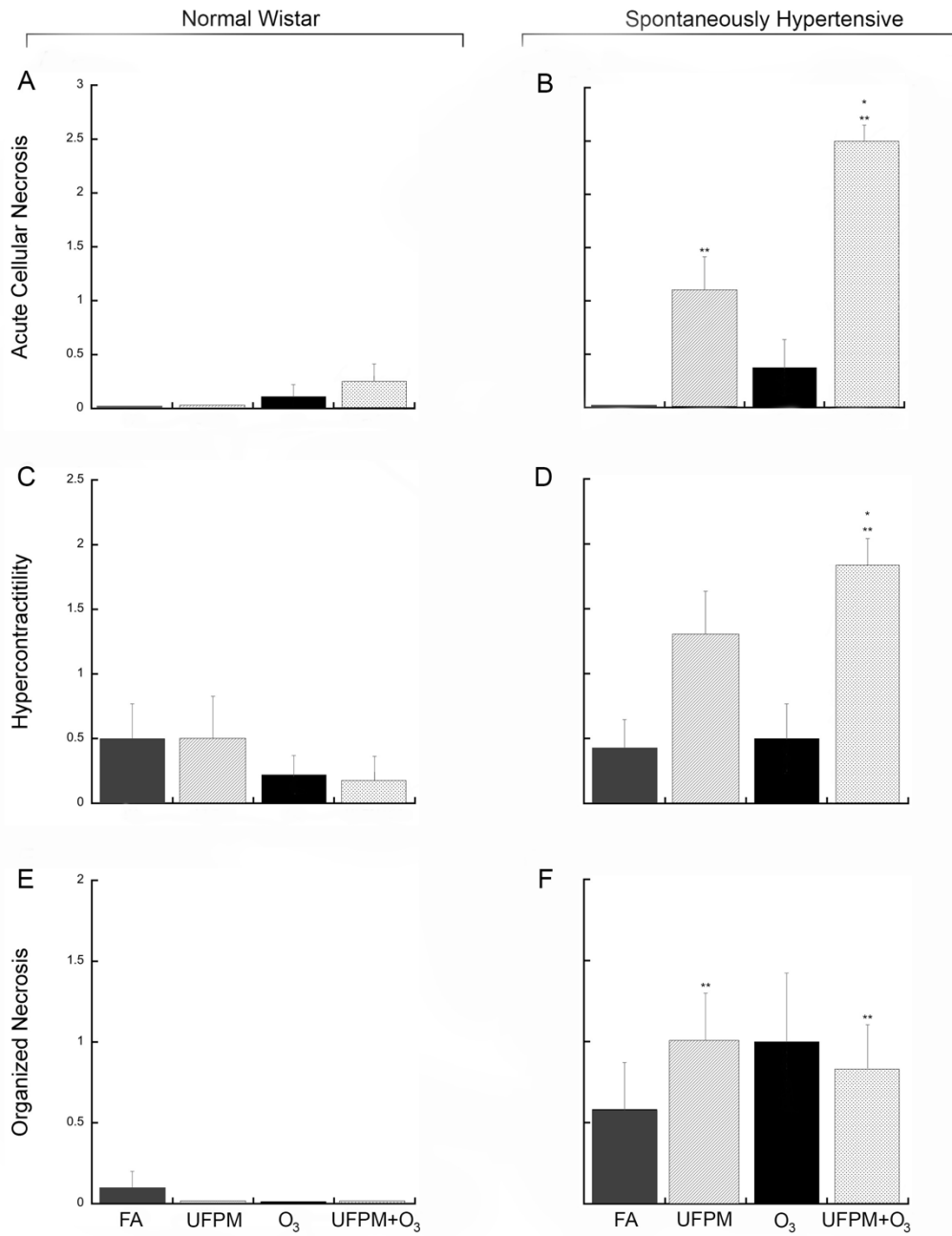
## Significant difference between NW and SH within same strain exposure groups.

### Cardiac Histopathology:

*Differences between strains.* Cardiac histopathology was analyzed by exposure group and strain. There were significant differences between the NW and SH strains in response to UFPM and UFPM+O<sub>3</sub>. Within UFPM exposure groups, there were significant differences between SH and NW rats for acute cellular necrosis (*p*=0.034) and organized necrosis (*p*=0.034). There were significant differences between SH and NW rats in response to UFPM+O<sub>3</sub> exposure for all three parameters; acute cellular necrosis (*p*=0.000), hypercontractility (*p*=0.000), and organized necrosis (*p*=0.044).

*Differences in response to exposure.* Within the NW rats there were no significant differences between the exposure conditions for any of the three parameters; acute cellular necrosis, hypercontractility or organized necrosis. In SH rats, there were significant differences with UFPM+O<sub>3</sub> for acute cellular necrosis in comparison with FA (*p*=0.000), UFPM (*p*=0.045), and O<sub>3</sub> (*p*=0.001). There was significant cardiac pathology for the SH rats between the different exposures. Significant differences in acute cellular necrosis were seen between all of the exposures. UFPM+O<sub>3</sub> was significantly different from FA (*p*=0.000), from O<sub>3</sub> (*p*=0.001) and from UFPM (*p*=0.045). Differences for hypercontractility between FA and UFPM+O<sub>3</sub> (*p*=0.002), and between O<sub>3</sub> and UFPM+O<sub>3</sub> (*p*=0.018). There were no differences in organized necrosis between any of the exposure conditions.

Figure 20. Acute Cellular Necrosis; Hypercontractility and Organized Necrosis.



## Summary and Conclusion:

The epidemiologic data from many parts of the world have shown that in aged populations, the people most at risk from exposure to severe air pollution are those with pre-existing cardiovascular disease. We wanted to understand the kinds of physiologic underpinnings of these observations, particularly with regard to changes in the peripheral blood, heart and lung when mature adult rats, with and without underlying cardiovascular disease were exposed to filtered air (control), ozone, particulate matter or a combination of ozone and particulate matter. Our studies demonstrated that:

- Ozone in combination with combustion derived ultrafine particulate matter produce a potentially more toxic profile of oxidant derived reaction products.
- Mature adult animals with cardiovascular disease are more susceptible to oxidant injury induced by ozone compared to age matched animals without cardiovascular disease as indicated by greater inflammation, airway injury and alterations in heart rate variability.
- The **co-pollutant ozone and ultrafine particulate matter** atmosphere induces significantly greater changes in airway injury, inflammation, alterations of heart rate variability, and arrhythmias than ozone or ultrafine particulate matter atmosphere alone in **mature adult animals with or without cardiovascular disease**.
- The co-pollutant ozone and ultrafine particulate matter atmosphere induces significantly greater changes in platelet activation, platelet microvesicles as well as platelet-white blood cell aggregates. These parameters lay the foundation for a pro-coagulant and pro-inflammatory systemic vascular environment.
- **Mature adult animals with cardiovascular disease** exposed to the co-pollutant ozone and ultrafine particulate matter atmosphere **develop myocardial injury** despite having similar changes in heart rate variability, and arrhythmias as age matched animals without cardiovascular disease.
- Evidence is consistent with an integrated response to the co-pollutant ozone and ultrafine particulate matter atmosphere that is initiated in the lung, results in downstream hematological and autonomic nervous system responses that manifest as increased arrhythmias, decreased heart rate variability and myocardial injury in mature adults with cardiovascular disease

These data strongly suggest that underlying cardiovascular disease in mature adult populations may be an important factor in the response to exposure to ozone as well as to ozone and ultrafine particulate matter.

**Recommendation:**

Findings obtained from our ongoing investigation, “Co-Exposure to PM and O<sub>3</sub>: Pulmonary C Fiber Platelet Activation in Decreased HRV”, demonstrate that exposure to a combination of ultrafine particulate matter (UFPM) and ozone (O<sub>3</sub>) has a synergistic effect, resulting in exaggerated patho-physiological responses compared to single pollutant exposure in mature adult rats. Importantly, these responses when present in a mature adult rat model of cardiovascular disease were associated with acute myocardial injury. This is the first study in an animal model to provide evidence of air pollution exposure-induced myocardial injury. Based on our current findings we recommend the following.

- Examine the mechanistic basis of the synergistic effects resulting from combined exposure to UFPM and O<sub>3</sub> in rats with and without cardiovascular disease.
- Define the effect of O<sub>3</sub> on particle distribution in the lung.
- Examine the distribution of pulmonary C fibers in the lung and their proximity to UFPM deposition.
- Determine whether UFPM+O<sub>3</sub> alters the expression of Nrf2-dependent phase II antioxidant enzymes.
- Define the effect of UFPM+O<sub>3</sub> on microthrombi in the pulmonary and cardiac vasculature.
- Characterize acute and chronic changes in the myocardium.

These types of studies will address some of the mechanisms behind adverse health effects of multi-pollutant exposure, in particular those associated with exposure to ambient air pollution and increased cardiac mortality in elderly individuals with underlying cardiovascular disease.

## References:

- Adar, S.D., Gold, D.R., Coull, B.A., Schwartz, J., Stone, P.H., Suh, H. 2007 Focused exposures to airport traffic particles and heart rate variability in the elderly. *Epidemiology* 18:95-103.
- Araujo, J.A., Barajas, B., Kleinman, M., Wang, X., Bennett, B.J., Gong, K.W., Navab, M., Harkema, J., Sioutas, C., Lulis, A.J., Nel, A.E. 2008 Ambient particulate pollutants in the ultrafine range promote early atherosclerosis and systemic oxidative stress. *Circulation Research* 102:589-596.
- Brook, R.D., Brook, J.R., Urch, B., Vincent, R., Rajagopalan, S., Silverman, F. 2002 Inhalation of fine particulate air pollution and ozone causes acute arterial vasoconstriction in healthy adults. *Circulation* 105:1534-1536.
- Brook, R.D., Franklin, B., Cascio, W., Hong, Y., Howard, G., Lipsett, M., Luepker, R., Mittleman, M., Samet, J., Smith, S.C., Tager, I. 2004 Air pollution and cardiovascular disease. A statement for healthcare professionals from the expert panel on population and prevention science of the American heart association.
- Delfino, R.J., Staimer, N., Tjoa, T., Polidori, A., Arhami, M., Gillen, D.L., Kleinman, M.T., Vaziri, N.D., Longhurst, J., Zaldivar, F., Sioutas, C. 2008 Circulating biomarkers of inflammation, antioxidant activity, and platelet activation are associated with primary combustion aerosols in subjects with coronary artery disease. *Environmental Health Perspectives* 116:898-906.
- Devlin, R.B., Duncan, K.E., Jardim, M., Schmitt, M.T., Rappold, A.G., Diaz-Sanchez, D. 2012 Controlled exposure of healthy young volunteers to ozone causes cardiovascular effects. *Circulation* 126:104-111.
- Fan, Z.T., Meng, Q., Weisel, C., Laumbach, R., Ohman-Strickland, P., Shalat, S., Hernandez, M.Z., Black, K. 2009 Acute exposure to elevated PM<sub>2.5</sub> generated by traffic and cardiopulmonary health effects in healthy older adults. *J. Exposure Science and Environmental Epidemiology* 117:105-111.
- Gold, D.R., Litonjua, A., Schwartz, J., Lovett, E., Larson, A., Nearing, B., Allen, G., Verrier, M., Cherry, R., Verrier, R. 2000 Ambient pollution and heart rate variability. *Circulation* 101:1267-1273.
- International Task Force. 1996 Heart rate variability. Standards of measurement, physiological interpretation, and clinical use. *Eur Heart J* 17:354-381
- Lee D, Wallis C, Wexler AS, Schelegle ES, Van Winkle LS, Plopper CG, Fanucchi MV, Kumfer B, Kennedy IM, Chan JK. 2010 Small particles disrupt postnatal airway development. *J Appl Physiol* 109(4):1115-1124.
- Littell, R.C., Henry, P.R., Ammerman, C.B. 1998 Statistical analysis of repeated measures data using sas procedures. *J Anim Sci* 76:1216-1231
- Lown B, Calvert C, Armiton R. 1975 Monitoring for serious arrhythmias and high risk of sudden death. *Circulation* 52(suppl 3):189-198.
- Lucking A.J., Lundback, M., Mills, N.L., Faratian, D., Barath, S.L., Pourazar, J., Cassee F.R., Donaldson, K., Boon, N.A., Badimon, J.J., Sandstrom, T., Blomberg, A., Newby, D.E. 2008 Diesel exhaust inhalation increases thrombus formation in man. *Eur. Heart J.* 29:3043-301.
- Malik, M. 1996 Heart rate variability. *Annals of Noninvasive Electrocardiology.* 1:1542-47.
- Norris, J.W., Pratt, S.M., Auh, J.H., Wilson, S.J., Clutter, D., Magdesian, K.G., Ferraro, G.L., Tablin F. 2006 Investigation of a novel, heritable bleeding diathesis of thoroughbred horses and development of a screening assay. *J Vet Intern Med* 20:1450-1456.
- Oberdorster, G., Sharp, Z., Atudorei, V., Elder, A., Gelein, R., Lunts, A., Kreyling, W., Cox, C. 2002 Extrapulmonary translocation of ultrafine carbon particles following whole-body inhalation exposure of rats. *J Toxicology and Environmental Health* 65:1531-1543.
- Peters, A., Dockery, D.W., Mueller, J.E. Mittleman, M.A. 2001. Increased particulate air pollution and the triggering of myocardial infarction. *Circulation* 103:2810-2815.

Pieters, N., Plusquin, M., Cox, B., Kicinski, M., Vangronsveld, J., Nawrot, T.S. 2012. An epidemiological appraisal of the association between heart rate variability and particulate air pollution: a meta-analysis. *Heart* 98:1127-1135.

Pino, M.V., Levin, J.R., Stovall, M.Y., Hyde, D.M. 1992. Pulmonary inflammation and epithelial injury in response to acute ozone exposure in the rat. *Toxicol Appl. Pharmacol.* 112:64-72.

Pope, C.A., Hansen, M.L., Long, R.W., Nielsen, K.R., Eatough, N.L., Wilson, W.E., Eatough, D.J. 2004 Ambient particulate air pollution, heart rate variability, and blood markers of inflammation in a panel of elderly subjects. *Environmental Health Perspectives* 112:339-345.

Samet, J.M., Dominici, F., Currier, I., Coursac, I., Zeger, S.L. 2000 Fine particulate air pollution and mortality in 20 U.S. cities, 1987-1994. *New England Journal of Medicine* 343:1742-1749.

Schelegle, E.S., Alfaro, M.F., Putney, L., Stovall, M., Tyler, N., Hyde, D.M. 2001 Effect of C-fiber-mediated, ozone-induced rapid shallow breathing on airway epithelial injury in rats. *Journal of Applied Physiology* 91:1611-1618.

Tablin, F., den Hartigh, L.J., Aung, H.H., Lame, M.W., Kleeman, J.F., Ham, W., Norris, J.W., Pombo, M., Wilson, D.W. 2012 Seasonal influences on CAPs exposures: differential responses in platelet activation, serum cytokines and xenobiotic gene expression. *Inhalation Toxicology* 24:506-517.

Tarvainen, M., Laitinen, T., Lipponen, J., Cornforth, D., Jelinek, H. 2014 Cardiac autonomic dysfunction in type 2 diabetes – effect of hyperglycemia and disease duration. *Front Endocrinol (Lausanne)* 5:130.

Tarvainen, M., Georgiadis, S., Ranta-aho, P., Karjalainen, P. 2006 Time-varying analysis of heart rate variability signals with kalman smoother algorithm. *Physiol Meas* 27(3):225-239.

Tontodonati, M., Fasdelli, N., Dorigatti, R. 2011 An improved method of electrode placement in configuration lead ii for the reliable ecg recording by telemetry in the conscious rat. *Journal Pharmacological Toxicological Methods* 63:1-16.

Wilson, D.W., Aung, H.H., Lame, M.W., Plummer, L., Pinkerton, K.E., Ham, W., Kleeman, M., Norris, J.W., Tablin, F. 2010 Exposure of mice to concentrated ambient particulate matter results in platelet and systemic cytokine activation. *Inhalation Toxicology* 22:267-276.

**Abbreviations (in alphabetical order):**

Acid citrate dextrose – ACD  
Acute cellular necrosis – CAN  
Akaike information criterion (AIC)  
Analysis of variance – ANOVA  
Atrial Premature Complexes - APC  
Autoregression – AR  
Cardiovascular – CV  
Complete Atrioventricular Block - 3-AVB  
Fast Fourier Transfer - FFT  
Filtered Air - FA  
Fluorescein isothiocyanate – FITC  
Forward scatter – FS  
Heart rate variability – HRV  
Heart rate variability triangular index – HRVti  
High frequency – HF  
Hypercontractility – HC  
Infarct – INF  
Integrin  $\alpha 2\beta 3a$  – CD41/61  
Integrin  $\alpha M$  – CD11b  
Integrin  $\beta 2$  – CD18  
Low frequency – LF  
Normal Wistar – NW  
Ozone – O<sub>3</sub>  
Phycoerythrin – PE  
Polycyclic aromatic hydrocarbons – PAHs  
Polymorphic Ventricular Premature Complexes - P-VPCs  
Power spectrum density - PSD  
Pre-mixed flame particulates – PFP  
P-selectin – CD62P  
Root mean square of successive RR interval differences - RMSSD  
Schwarz Bayesian criterion – SBC  
Second Degree Atrioventricular Block - 2-AVB  
Side scatter - SS  
Spontaneously Hypertensive - SH  
Standard deviation of normal-to-normal RR intervals – SDRR  
Supraventricular Couplet - SV-Couplet  
Supraventricular Tachycardia – SVT  
Supraventricular Triplet - SV-Triplet  
Triangular interpolation of RR interval histogram – TINN  
Ultrafine particulate matter – UFPM  
Ventricular Couplets - V-Couplet  
Ventricular Premature Complexes - VPC  
Ventricular Tachycardia - VT  
Ventricular Triplets- V-Triplet  
White blood cell - WBC